Theses and Dissertations

May 2019

Integration of Preventive and Emergency Responses to Boost Distribution System Resilience

Gang Wang
University of Wisconsin-Milwaukee

INTEGRATION OF PREVENTIVE AND EMERGENCY RESPONSES TO BOOST

DISTRIBUTION SYSTEM RESILIENCE AGAINST WINDSTORMS

by

Gang Wang

A Thesis Submitted in

Partial Fulfillment of the

Requirements for the Degree of

Master of Science

in Engineering

at

The University of Wisconsin-Milwaukee

May 2019

ABSTRACT

INTEGRATION OF PREVENITVE AND EMERGENCY RESPONSES TO BOOST
DISTRIBUTION SYSTEM RESILIENCE AGAINST WINDSTORMS

by

Gang Wang

The University of Wisconsin-Milwaukee, 2019
Under the Supervision of Dr. Lingfeng Wang

Recent years have seen a series of large-scale blackouts due to extreme weather events around the world. These high impact, lower probability events have caused great economic losses to modern society. Therefore, it is urgent to study the resilience improvement measures of power systems to mitigate the effects of adverse extreme events. Current research mainly focuses on the hardening measures where robust optimization is used to solve the problems. However, due to the consideration of worst case of uncertain parameters, the robust optimization method is usually too conservative and uneconomical in many situations.

In this thesis, operational measures are deployed to boost the distribution system resilience considering all possible scenarios. An integrated resilience response framework is proposed, which provides distribution system operators solutions to address the resilience enhancement problem in both preventive state and emergency states. The key of the framework is a two-stage stochastic mix-integer linear optimization model. The mathematical formulation and the solving method, progressive hedging algorithm, are presented in this thesis as well. Preventive response

includes topology reconfiguration and generator redispatch, while topology reconfiguration, generator redispatch and load curtailment are allowed in emergency response.

Case study on IEEE 33 bus system and a modified 69 bus system validates the correctness and effectiveness of the proposed framework and model. Integrated response solution is obtained by solving the model and sensitivity analysis is performed to study the performance of integrated response under different system parameters. The key conclusions include the following: 1) integrated response improve distribution system resilience in a minimum cost; 2) integrated response is preferable to either individual preventive or emergency response; 3) system parameters and abilities such as unit load shedding cost, ramping ability and generator availability influence the system resilience and expected total cost in different degrees.

TABLE OF CONTENTS

LIST OF FIGURES

LIST OF TABLES

NOMENCLATURE

Sets and Indices

L Sets of distribution lines indices (i,j)

S Sets of possible scenarios indices s

B Sets of buses indices I

DB Sets of buses with demand

GB Sets of buses with distributed generators

SL Sets of lines with switches

G Sets of distributed generators indices g

Parameters

$y^0_{i,}$ Parameter indicating initial line status of line (i,j) closed (1) or not (0)

$y^b_{i,j}$ Binary parameter indicating damage status of line (i,j) damaged (0) or functional (1)

c^{shed}_i Penalty cost ($) for shedding 1 kWh load at bus i

ω_s Probability that scenario s happens

P^d_i Active load demand at bus i

Q^d_i Reactive load demand at bus i

$G_{i,j}$ Conductance of line (i,j)

$B_{i,j}$ Susceptance of line (i,j)

P^{min}_g Minimum output of generator g

P^{max}_g Maximum output of generator g

$P^{max}_{i,j}$ Maximum line capacity of line (i,j)

V^{min}_i Minimum voltage magnitude at bus i

V^{max}_i Maximum voltage magnitude at bus i

$P^{rp,max}_g$ Maximum ramping rate of generator g

Δt Times period duration interested

Variables

$y^a_{i,j}$ Binary variable indicating whether line (i,j) is closed (1) or not (0) after preventive measures employing

$P^{c,s}_{shed}$ Load shedding in scenario s

P^a_g Active power output of generator g after preventive measures

Q^a_g Reactive power output of generator g after preventive measures

$P^a_{i,j}$ Active power flow of line (i,j) after preventive measures

$Q^a_{i,j}$ Reactive power flow of line (i,j) after preventive measures

V^a_i Voltage magnitude at bus i after preventive measures

$\theta^a_{i,j}$ Voltage angle deviation of bus i and j after preventive measures

$\beta^a_{i,j}$ Binary variable equals 1 if j is the parent bus of i and 0 otherwise

$y^{c,s}_{i,j}$ Binary variable indicating whether line (i,j) is closed (1) or not (0) after emergency measures employing in scenario s

$P^{c,s}_g$ Active power output of generator g after emergency measures in scenario s

$Q^{c,s}_g$ Reactive power output of generator g after emergency measures in scenario s

$P^{c,s}_{i,j}$ Active power flow of line (i,j) after emergency measures in scenario s

$Q^{c,s}_{i,j}$ Reactive power flow of line (i,j) after emergency measures in scenario s

$V^{c,s}_i$ Voltage magnitude at bus i after emergency measures in scenario s

$\theta^{c,s}_{i,j}$ Voltage angle deviation of bus i and j after emergency measures in scenario

ACKNOWLEDGEMENTS

I would like to express my appreciation to my advisor, Dr. Lingfeng Wang, for encouraging and guiding me to conduct in-depth research about power system. Dr. Wang has a comprehensive understanding of the power system and related topics. He teaches me to devote myself in academic research to make progress. And he is willing to take the time to guide us technically. I am very grateful. He always asks me to further the research and focus on the results which are contradictory with existing theories or practices. It is the source of new discoveries.

I would also like to extend my thankful gratitude to my thesis committee members, Dr. Weizhong Wang and Dr. Wei Wei. Thank you for your time and effort and thank you for letting my defense be an enjoyable moment. Thank you for your brilliant comments and practical suggestions.

I would also like to thank Dr. Zhaoxi Liu and Dr. Li Ma. They provide me lots of suggestions and advice to enable my research progress. Their devotion to academic research touched me deeply.

And special thanks to my family for supporting me. Their love and care are always with me.

Chapter 1 Introduction

1.1 Background

Recent years have seen the great impact of extreme weather events on the global power system because of climate change, and the frequency and intensity of natural disasters are expected to increase in the future [1]. The occurrence of extreme weather events can lead to massive power outages and economic losses. Distribution systems are especially influenced by extreme weather events due to line damage, effects of radial topologies and limited backup resources.

For instance, Hurricane Wilma have caused more than $27.4 billion in Cuba, Mexico and Florida, of which $19 billion happens in the United States [2]. In 2008, a severe ice storm in China caused 2,000 substations failure and 8,500 towers collapsed and more than 170 cities suffered power outages. Besides, Hurricane Sandy happened in October 2012 caused damage to power system in New York city, and the city power supply was cut off [3]. Actually, there is evidence that 80% ~ 90% of large power outages come from distribution system failures [4].

Most existed power distribution systems are designed and maintained within the framework of safety and sufficiency in reliability principle, which perform well in normal weather conditions but not in severe natural disasters. To cope with the great challenge of high impact low probability (HILP) extreme weather issues such as hurricanes and windstorms, the concept of power system resilience should be explored and stressed.

There is no agreement yet on the resilience definition. If the power system is

capable of preparing, absorbing, adapting, and quickly recovering from adverse events, it is defined to be resilient [5]. The focus of resilience is the ability of adaptation and recovery towards natural disasters. Here, "adaptation" refers to the process of system changing to better adapt to new operation environment, and "recovery" means the process of recovery of a system to its initial operation state after a disturbance or break. Besides, system resilience level is adaptive, ongoing and differs in short and long term, concentrating on the whole process of system under a specific disaster, while reliability is static, time-invariant and without event sensitivity.

Power system resilience improvement measures is classified as hardening-oriented and operational methods [6]. Hardening-oriented methods mainly focus on improving the performance of power system infrastructure component under extreme events such as elevating substations, plant management and new component installment. They are regarded as more passive and expensive, compared to operation-oriented measures, and involve long term action. Operational measures are relatively active and affordable, which are always associated with short-term or real-time decision and responding. Distributed energy system, demand side management, network reconfiguration and microgrids are the mainly operational measures. According to the three operating states that power systems go through in an event, operational resilience improvement measures can be classified into the three categories [7]. As a consequence, there are four categories of resilience improvement measures totally, as depicted in **Figure 1.1**.
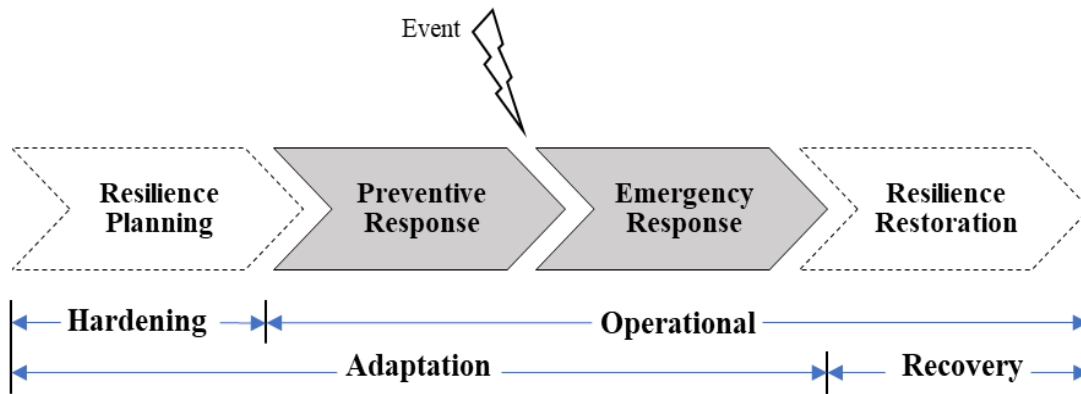
Figure 1.1 The resilience enhancement steps [8] and the scope of this thesis (shaded).

1.2 Problem Description

The thesis aims to boost distribution system resilience by enhancing the system adaptability and operational measures. Therefore, only preventive response and emergency response are included (shaded in **Figure 1.1**).

In general, preventive responses include actions taken prior to the occurrence of a disaster, while emergency responses are utilized after an extreme event. To make the problem simple, only generators, distribution lines, loads in distribution systems are taken into consideration in this thesis. Accordingly, the specific resilience improvement approach will include generator redispatch, topology reconfiguration and load shedding. Load shedding is not included in preventive response since distribution systems should operate in normal condition to supply all the loads when meet all operation constraints in preventive state. Generator redispatch and topology reconfiguration are available in both pre-event state and post-event state to maximize the benefits. Besides, the effectiveness of integrated response is always better than deploying single emergency or preventive response.

Existed resilience improvement research mainly focus on hardening measures in

resilience planning and robust method is deployed in solving such problems. Robust method regards the worst-case solution as the global solution. Sometimes they are too conservative and the expected economic loss is over-estimated. As to operational problem, there is no current research using stochastic method to improve system resilience where topology reconfiguration is allowed in both preventive and emergency responses.

To further enhance the distribution system resilience, the thesis aims to find the integration of preventive response and emergency response (called integrated response in the thesis) to boost distribution system resilience against windstorms in a minimum cost. The preventive response includes generator redispatch and topology switching, while the emergency response involves generator redispatch, switching and load shedding. The uncertainty of component damage status after windstorms is considered by using the fragility curves and finding solution for all possible scenarios in a probabilistic way.

1.3 Contribution

- Review the literature on power system resilience in detail
- Propose a two-stage integrated response framework with integration of preventive response and emergency response to boost distribution system resilience against windstorms
- Formulate the core of integrated response framework in a two-stage stochastic mix-integer linear model
- Illustrate the effectiveness of proposed approach in case study

1.4 Thesis Structure

Chapter 2 gives a literature review on power system resilience from the perspective of resilience definition, evaluation methods and metrics and improvement measures. A chosen has been made between stochastic method and robust method.

Chapter 3 first proposes a two-stage integrated response framework to enhance system resilience. Then the concept of fragility curves and scenarios are introduced to carry out stochastic calculation. The outline of the two-stage model is presented in mathematical way, so as the solving method, the progressive hedging method.

Chapter 4 introduces the mathematical formulation of the two-stage stochastic model. The linearization procedure and the detailed solving method is presented.

Chapter 5 provides case study in IEEE 33 bus system and a modified 69 bus system to illustrate the correctness and effectiveness of proposed framework and model. Sensitivity analysis about unit load shedding cost, ramping ability and generator availability is conducted to investigate the impact of parameters to the system resilience level and expected total cost.

Chapter 6 makes a conclusion of the thesis and future work is discussed.

Chapter 2 Resilience Related Literature Review

In this chapter, the definition of power system resilience by different organizations and authors is first presented. Then the evaluation methods and metrics to power system resilience are listed by reviewing relative papers. Finally, the resilience improvement measures are collected, which could be divided into three categories, preventive measures, emergency measures and restoration measures.

2.1 Definition

In the past few decades, many natural disasters have occurred under the influence of global climate change, resulting in large-scale blackouts and property losses around the world. Specifically, extreme weather events have caused 80% of the power loss in U.S between 2003-2012 and cost billions of dollars every year [9]. These high impact low probability (HILP) events have drawn people's great attention to the concept of power system resilience.

"resilio" is the original of the word "resilience". It refers to the ability to jump or rebound or rebound and contract. If the power system is capable of preparing, absorbing, adapting, and/or quickly recovering from adverse events, it is considered to be resilient [5]. However, the first definition of resilience appeared in ecological system by Holling in 1972 [10], which is described as "measure of the persistence of systems and of their ability to absorb change and disturbance and still maintain the same relationships between populations or state variables". Since then, the concept of resilience was widely adopted in many research fields such as economy, urban planning, psychology, engineering and construction, energy development, materials science, control systems,

etc.

The "adaptation" and "recovery" words are quite commonly used in over 70 definition of resilience. Power system resilience is regarded as a typical feature of modern power system in 2009 [11]. Resilience is defined as "the ability to prepare for and adapt to changing conditions and withstand and recover rapidly from disruptions" [12]. The UK Energy Research Centre (UKERC) sees resilience as "the ability of energy systems to tolerate interference and continue to provide consumers with affordable energy services" [13]. Power system resilience can be also used to describe the ability of a system, community or society [14]. M Panteli. links long-term resilience with system planning and adaptation capacity, while short-term resilience is the system resilience performance before, during and after an event [6]. Relatively, the two main characteristic in power system reliability is "security" and "adequacy", and reliability is defined as the system ability to satisfy its load demand under the specified operating condition.

Extreme Weather Events → Infrastructure Component Failure → Bad Performance of System Operation
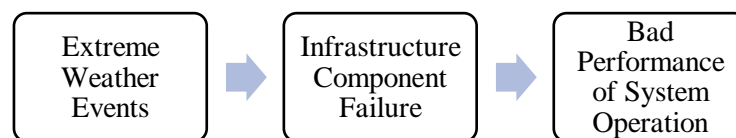
Figure 2.1 The intrinsic logic of events and its impact.

Most extreme weather events affect the overall performance of power systems by affecting the effectiveness of infrastructure such as transmission line failure and generator outage. Power system resilience not only involves component failure under extreme events, system operation condition also accounts. **Figure 2.1** indicates the intrinsic logic of extreme events and its impact to power systems.
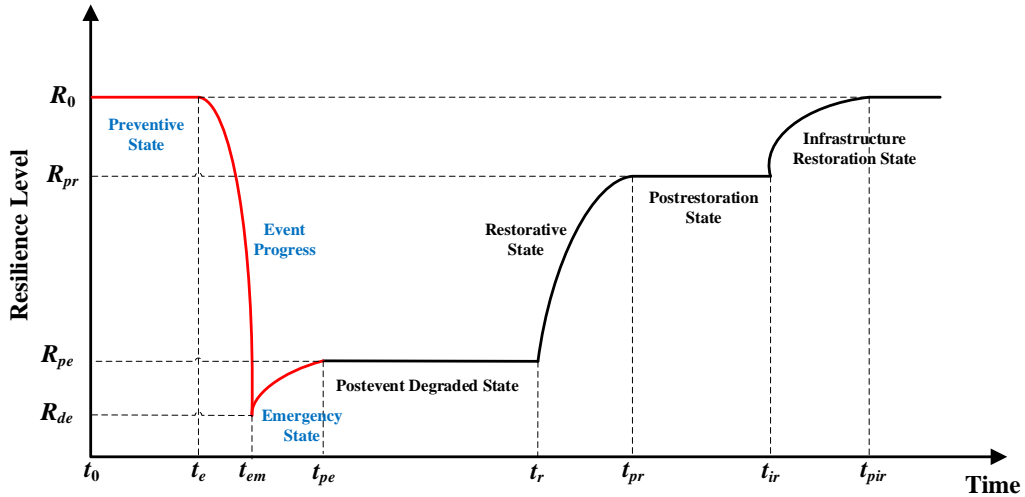
Figure 2.2 An example of distribution system resilience level under an event [15].

Based on this intrinsic logic, a distribution system resilience curve associated with an event is shown in **Figure 2.2** [15]. The red part is the phases focused on including preventive state, event progress and emergency state. The system overall resilience level is the function of time for a disturbance event. A resilient power system needs to be robust and resistant at preventive state when the preventive measures are employed and the resilience level is R_0. System in that period is strong enough to defense the upcoming extreme events partly or totally with its robust component and structure. After the event occurrence time t_e, the system resilience level goes through a huge decline to a post-event level R_{de}. Due to the small geographic dimension of distribution system, the duration of event progress t_{em}-t_e is within several minutes or hours. The system goes through an emergency state right after the event leaves, when the emergency measures and correct actions are implemented and resilience level goes from R_{de} to R_{pe}.

Time period between t_{pe} and t_r is used to prepare for the next restorative step. Resourcefulness and redundancy are the key characteristic in the degradation state, which helps to minimize the resilience degradation R_0-R_{pe} and the restoration preparing

time t_r-t_{pe}, since resourcefulness and redundancy in system component, power supply and people can provide flexibility to the system to deal with the disturbance event.

The system enters into restorative state after t_r, during which all the possible recovery operations are put into effect such as component fixing, generator redispatch, demand side management and topology reconfiguration. The key issue in this state is the system recovery ability to help the system resilience level recover to R_{pr}. Notice that in most cases $R_{pr} < R_0$. Due to the system redundancy, the system may have recovered to its initial operation condition (operational resilience) when not all of the infrastructure is repaired (infrastructure resilience). Usually it takes more time to get infrastructure fully recovered than it comes to system operation condition, which can be represented by $(t_{pir}$-$t_{ir}) > (t_{pr}$-$t_r)$.

The resilience level has different meanings. Total load supplied, voltage and frequency performance can act as operational system resilience performance, while number of transmission lines in service is one of the infrastructure resilience performance. It is hard to evaluate a system resilience with only one particular index, such as resilience level or transaction times between different resilience states. However, with the perspective of "adaptation" and "recovery", the most important metrics in **Figure 2.2** are the resilience degradation R_0-R_{pe} and the operational response/recovery time t_{pr}-t_r. And the details of resilience evaluation methods and metrics will be discussed in the next section. Besides, it is worth mentioning that the restoration time depends on not only the severity of events, but also the system resilience performance before, during, and after the disturbance or break.

Based on above illustration, the power system resilience definition in [8] is adopted in this thesis. System resilience is seen as the power system adaptability to natural disasters and the recover ability to initial operation states.

2.2 Evaluation Methods and Metrics

Power system resilience is time-varying and event-varying, which indicates that resilience has to be evaluated in multidimensional way with respect to a specific event. In power system engineering risk evaluation, the traditional way is to calculate the reliability indices such as expected energy not supply (EENS), loss of load probability (LOLP), loss of load frequency (LOLF) and system average interruption duration index (SAIDI), system average interruption frequency index (SAIFI). They are used for distribution system particularly. Unlike the metrics in reliability evaluation, there is yet no widely agreed metrics in resilience assessment. Existed resilience evaluation approaches are divided into two categories: qualitative approaches and quantitative approaches [16]. **Figure 2.3** is a summary of these approaches.
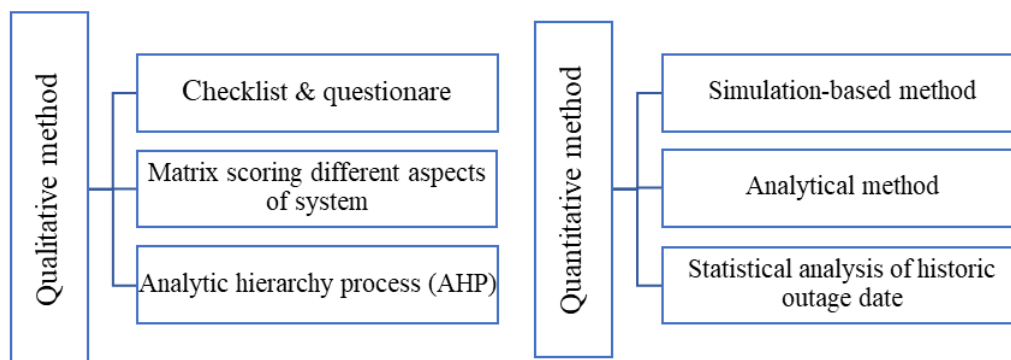
Figure 2.3 Summary of resilience evaluation methods [16].

2.2.1 Qualitative Methods

It is seen that the qualitative resilience assessment approaches contain three types: the checklist & questionnaires, matric scoring different aspects of system and analytic hierarchy process. For instance, checklist and questionnaires are used in [17] to provide measurement of resilience at all levels, critical infrastructure, community, and region level. Business structure such as supply chain and governance subsystem is addressed to better evaluate community and region resilience. A complete resilience matrix is concluded in [18] where both physical resilience and information resilience are explored. In [19], analytic hierarchy process is used to explore the criteria to evaluate the risk of power system in the Philippines. Qualitative methods in resilience assessment can help energy policy makers to make long-term decision considering the future development and resilience of local power system.

2.2.2 Quantitative Methods

Simulation, analytical approach and historic data analysis are the main approaches in quantitative methods in resilience evaluation. Similar to counterpart methods in reliability evaluation, simulation-based methods are more applicable for complex systems due to the strong applicability and fixed process. Analytical methods are preferred for small-scale power systems because they are simple and computational efficient.

Monte Carlo simulation (MCS) is a simulation method, which is always used to evaluate the risk level of a specific event or a system and the uncertainty of parameters can be considered by repeated experiment. MCS is used in [20], [21] and [22] to evaluate power system resilience level. Based on sequential MCS, [20] explores the

influence of uncertainty of weather events such as weather intensity and duration to power system reliability metrics through a new reliability model. Reference [21] does a probabilistic modeling and MCS is used to speed up the assessment of component temperatures. Being capable of capturing the stochastic behavior and impact of windstorms, sequential MCS is also used in [22] to assess power system resilience.

Some papers use reliability indices directly to estimate system resilience level such as EENS [23], LOLE, LOLF [22]. Based on **Figure 2.3**, $TP(t)$ represents the resilience curve when there are no extreme weather events, and the resilience curve under event is expressed by $P(t)$, system resilience level $R(t)$ is calculated as (change T_{ir} to T_{pir} when it comes to infrastructure resilience) [24]:

$$R(t) = \frac{\int_0^{T_{ir}} P(t)dt}{\int_0^{T_{or}} TP(t)dt} \tag{2.1}$$

Reference [25] proposes an approach to investigate the performance of system infrastructure under natural disasters. Hurricane Katrina is examined to validate the proposed model in resilience improvement. Three typical resilience indices are defined in [26] by calculating the lost revenue impact (LRI), total restoration (TR) and recovery resilience (RR), based on which a framework for resilience analysis is proposed. Based on system resilience performance curve, reference [27] presents three ways to quantification the performance loss. Three other metrics, vulnerability index (VI), normalized index (DI), the restoration efficiency index (REI) and microgrid resilience index (MRI) are defined respectively with resilience indicators in different event stages [28]. Similarly, metrics presented in [29] describe power system infrastructure

resilience and operational resilience from four aspects, respectively. They are resilience degradation rate Φ, degradation level Λ in disturbance progress, the duration of post-event degraded state E and recover rate Π in restorative state.

In recent research, the majority of the resilience evaluation methods in power systems under extreme weather events are analytical methods. Power system resilience performance curve is essential in analytical resilience evaluation, and most of the metrics are mathematical description of the resilience curve towards a specific event.

Statistical analysis of historic data is commonly employed when repeated disturbances or shocks occur in same area. In [30], the outage data for three cities in previous four years are used to estimate the outage duration for distribution system. The outage data in Hurricane Katrina 2005 in Louisiana, Alabama, and Mississippi are collected and analyzed to assess system resilience level after the resilience improve measures [25].

They key issue of the thesis is not distribution system resilience evaluation, but the improvement measures which help to enhance power system resilience by reducing the damage of natural disasters. Thus, the expected amount of load curtailment after events is calculated to assess the effectiveness of proposed measures. The less the load curtailment is, the better the measures are.

2.3 Improvement Measures

Power system resilience evaluation is the foundation of resilience improvement measures, for it can give objective evaluation to the effectiveness of a proposed improvement measure, even system parameters and states can be optimized based on

evaluation metrics. Modern technologies such as smart grid and automation help to increase the diversity of resilience improvement measures in reduce the influence of natural disasters towards power system.

Many literatures have divided resilience improvement measures into several categories according to different criteria. Reference [22] classifies improvement measures as long-term improvement measures and short-term measures. Long-term measures involve planning, construction, maintaining, and upgrading, while short-term measures include black-start capabilities, generator redispatch, demand side management, emergency strategies. They can be carried out before, in and after a specific natural disaster according to their action time. A widely accepted indication is to category resilience enhancement measures into hardening and operational measures [6].

2.3.1 Hardening Measures

System hardening is to harden the system infrastructure with robust materials to reduce the damage of natural disasters such as earthquake, windstorms and hurricanes [31]. Hardening measures aim to boost infrastructure resilience by using strong materials in infrastructure construction, plant management, new system component installment and component movement, which are all changed in a physical way to make system more resilient to extreme weather events. They are regarded as more passive and expensive, compared to operation-oriented measures, and they involve long term action.

Several researches have been carried on in system hardening focusing on line hardening and switching installment using optimization techniques. Optimal hardening plan and operation condition is obtained by solving a two-stage robust optimization problem in reference [32]. Reference [33] presents a two-stage tri-level robust optimization problem to get optimal gas and power system hardening and installment plan considering the uncertainty in natural disasters. Stage one determines the installment strategy of new component and stage two is used to get optimal operation variables. Reference [34] obtains optimal resilience improvement plan in a two-stage robust problem. The optimal system construction plan is obtained and the model is examined through two test systems.

Reference [35] formulates a robust trilevel model to boost system resilience, in which microgrids are formulated and distribution lines are hardened. The total cost includes system hardening cost and operation cost. The uncertainty of renewable energy is taken into consideration in a stochastic way. Reference [36] explores the effectiveness of hardening measures in gas and power system by proposing a trilevel robust optimization problem. The worst scenario is identified and optimized with the metrics of load curtailment cost. And Reference [37] proposes a tri-level model to boost distribution system resilience by minimizing the total cost, where upgrading distribution poles, vegetation management and the combination of them are considered.
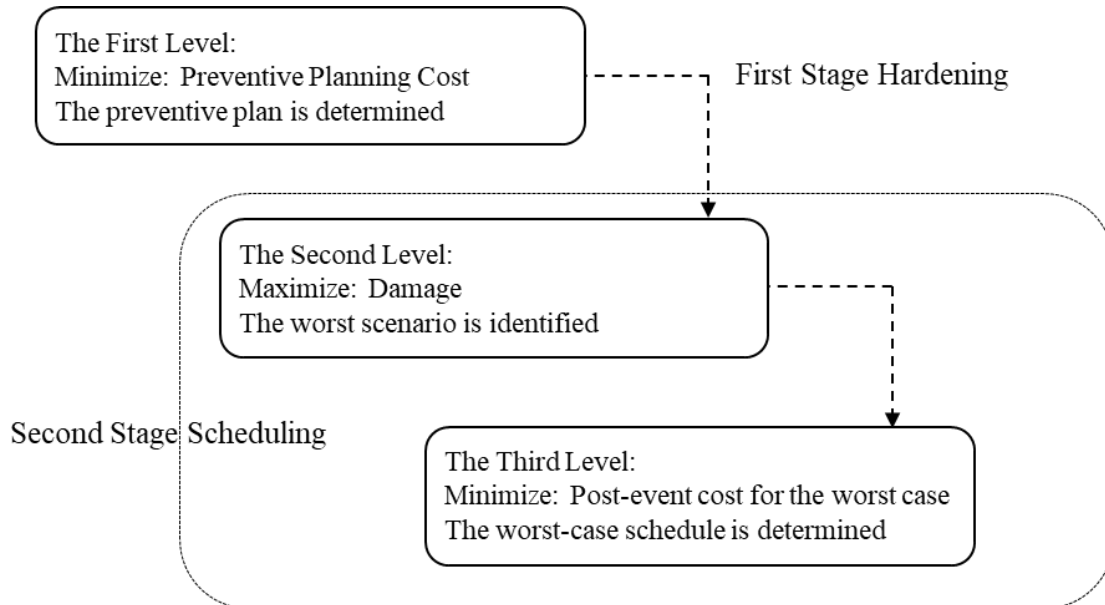
Figure 2.4 Typical two-stage trilevel model for preventive hardening problem.

We can see that robust two-stage problem and tri-level robust optimal model are widely used in line hardening problem. The three layers of model correspond to the three stages of an extreme weather event (see **Figure 2.4**). System operators have to make decisions before the event come, such as network reconfiguration and line hardening strategy, which corresponds to the preventive stage in **Figure 2.2**. Then the event comes and the system suffers from outages and damages. The damage is maximized in the second layer of the model to consider the worst case, which happens in the event progress. And the responding action is modeled in the third layer to mitigate the impact of the event. The above correspondence reflects the adaptability of the tri-level model in extreme events. Emergency responses and restoration measures can be both employed in the third level.

Advanced switching placement can also provide flexibility for power system faced with a natural disaster in both in pre-event state and post-event state. Reference [38] aims to enhance distribution system resilience by installing new switch and load

curtailment. *N*-1 and *N*-2 scenarios are considered and load restoration are carried out with priority. Reference [39] optimizes the location of new installed switch in distribution systems by minimizing the construction cost and load shedding cost. Two case studies show the efficiency and effectiveness of switch placement in boosting distribution system resilience.

2.3.2 Operational Measures

The operational methods enhance power system operational resilience by providing overall flexibility, efficiency when faced an up-coming extreme weather event. Operational measures focus on improving the system operational performance, including distributed energy systems, demand and generator management, topology reconfiguration, preventive control, accurate situation awareness, microgrids formulation, advance and quick recovery, etc. They are relatively active and affordable, which are always associated with short-term or real-time decision and responding.

Among the operational measures, transmission and distribution lines reconfiguration can provide flexibility to bulk power systems and distribution networks to mitigate the damage when a disturbance event occurs. Topology reconfiguration and microgrids formulation are the main methods in switching-involved resilience improvement measures.

Topology reconfiguration is a widely employed resilience improvement measure for it can maintain power system operation while minimize the system loss. The working mechanism of reconfiguration in extreme events are shown in follows.
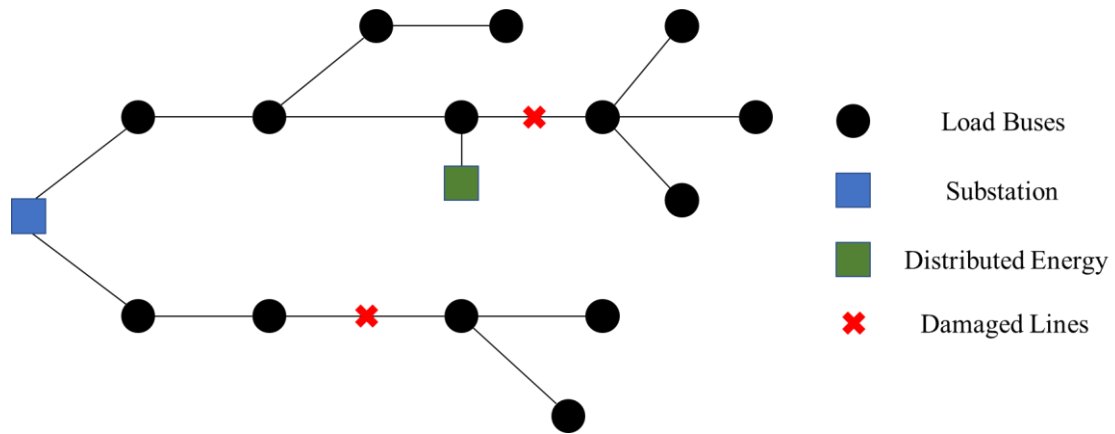
Figure 2.5(a) Distribution System Topology after natural disasters.
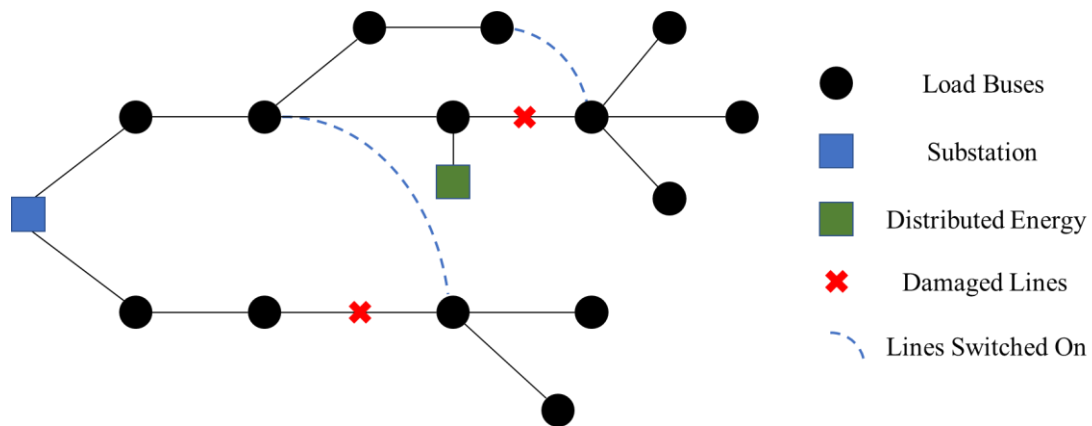
Figure 2.5(b) Distribution System Topology after switching reconfiguration.

Natural disasters cause great damage to power systems, especially distribution systems by destroying components such as lines and towers. **Figure 2.5(a)** is a distribution system topology after natural disasters. Two distribution lines failed and several load buses is separated from power sources. By doing topology reconfiguration, two tie-branches are switched on as the **Figure 2.5(b)** shows, and all the load buses are connected, which reduce the amount of load curtailment significantly. The distributed energy serves as controllable power resource to support the bus voltage. Topology reconfiguration is always employed in emergency state (see **Figure 2.2**).

For topology reconfiguration, reference [8] enhances bulk power systems with the

combination of preventive response and emergency response. Preventive response involves generator redispatch and topology reconfiguration. And emergency response not only included generator re-dispatch, topology reconfiguration but also load curtailment. Preventive topology switching and defensive islanding are employed in [40] to help to the formulation of multiple energy system island, which reduces the probability of cascading events caused by up-coming extreme weather events. A self-healing technique in proposed in [41] considering power resource availability, topology switching, and demand side management. Two case studies are carried to show the importance of reconfiguration in improving system resilience level.

For microgrids formulation, a proactive microgrids management method is proposed to reduce the microgrid vulnerability towards windstorms [42]. The load is fully supplied while the minimum amount of fragile lines is in service. In [43], the critical loads recover rapidly by topology reconfiguration and microgrids formulation. Distributed energy resources are attached in distribution systems and optimal operation condition is obtained by solving a mix-integer linear problem. Reference [44] presents four metrics to evaluate the severity of natural disasters and microgrids formulation is used to boost power system resilience. The Markov chain is used to represent the transaction between different system states and the uncertainty of event is modeled by doing Monte Carlo simulation. Microgrids formulation is mostly used in restoration state for load restoration.

To model the impact of natural disasters to power systems, accurate weather forecasting is also essential in the resilience improvement problem. Three categories of

environmental data need to be considered. The first one is system and geometric data such as system topology data, load data, initial system status, plant distribution data and terrain data [45]. System data is obtained by situational awareness. It is worth mentioning that situation awareness should be carried out all the time and once it is out of function partly or totally, the system may fail to respond to extreme conditions because the lack of accurate data [46]. Assume that system awareness is sufficient in the thesis. Wind speed is obtained by weather forecasting. It is demonstrated that natural disaster severity and parameters such as wind speed and area of influence make impact on the possibility of component damage [47]. Three metrics are introduced in [48] to evaluate the cost of operational measures.

There are also other resilience enhancing measures besides reconfiguration and some researches have been carried on to explore the measure beneficial to the restoration of power systems after a disturbance event. Mobile emergency resources and distributed energy can be utilized in extreme condition when normal power resources are disconnected from systems before or after the event.

Mobile emergency resources such as mobile generators and mobile storage units also help to reduce the operation cost when there is an extreme weather event. By the combination of preposition and rerouting of mobile resources, a tradeoff between expensive construction cost and low event probability is achieved. Mobile emergency resources are employed in [49] with topology reconfiguration and microgrids formulation, which reduces the power loss in critical load restoration procedure. Reference [50] involves not only mobile emergency generators preposition in the

preventive state but also emergency dispatching after the event. The problem is modeled as a two-stage stochastic optimization problem and solved by scenario decomposition algorithm. Similarly, reference [51] formulates a stochastic model combining preventive planning and real-time dispatching of mobile generators and storages to enhance distribution system resilience. Since topology reconfiguration is utilized in this study, multiple microgrids are formulated and the expected total cost is optimized. This research is also furthered by considering the total cost in normal operation state and the necessity of improving system resilience when it comes to severe weather-related events [52].

The effectiveness of distributed energy is illustrated in [53], [54] and [55]. Reference [53] uses photovoltaics generator and energy storage systems to enhance system resilience, where the optimal capacity and installment location of distributed energy is obtained. In [54], for the recovery of critical load in distribution system, DG are used in emergency state after an extreme disaster, boosting system resilience by reducing the amount of load curtailment in a period of time. Distributed energy is also used in [55] to minimize the duration of load shedding, while the optimal solution is obtained by solving a stochastic optimization problem.

2.3.3 Robust vs Stochastic

Based on previous literature review, it is concluded that there are two main categories in optimal resilience improvement problems, robust method and stochastic method. Robust methods are widely used in optimal hardening problems in [32][33][35][36] and [37], while stochastic methods are used in both hardening

problems [34][38][39] and operational problems [51][52]. Paper [8] employs robust method in operational problem, where topology reconfiguration, generator redispatch are used to enhance power grid resilience. However, the robust method only considers the worst case, in which the damage of windstorms is maximized. Therefore, the objective function value in robust optimization is larger than the stochastic method due to consideration of worst scenario instead of all possible scenarios. Stochastic optimization provides relatively accurate value for evaluating the effectiveness of proposed method in resilience improvement problem with acceptable computation burden. **Table 2.1** is a comparison between robust and stochastic method in resilience improvement problems.

Table 2.1 Comparison between robust and stochastic methods

	Robust Methods	Stochastic methods
Scenarios interested in	Worst case	All the scenarios
Where are the scenarios come from	Optimization	Scenario generation and reduction
Accuracy	Too conservative	Accurate
Computation burden	Relatively low	Relatively high
Mainly used in	Hardening problems	Hardening and operational problems

To make up with the disadvantage in robust method in integrated response problem, this thesis proposes an integrated response plan with combination of preventive response and emergency response to boost distribution system resilience against windstorms. A two-stage stochastic model is formulated where all the possible scenarios are considered and a global optimal solution is obtained.

2.4 Conclusion

This chapter provides a literature review about power system resilience. System resilience in this thesis is seen as the power system adaptability to natural disasters and the recover ability to initial operation states. Several resilience evaluation methods and metrics are then listed, and the expected amount of load curtailment after event is chosen as the resilience index in the thesis. In section 3, resilience improvement measures are introduced in the categories of hardening and operational measures. The comparison of robust and stochastic method is also given and the stochastic method is finally used to formulate the optimal operational method model.

Actually, the chosen of robust and stochastic methods is a tradeoff between computation burden and accuracy. Based on the consideration of all possible scenarios, the obtained decision variables in stochastic methods gives a global version of the problem solution, while robust methods are more conservative, in which the worst case is considered and the total cost is over-estimated.

The thesis aims to boost distribution system resilience by enhancing the system adaptability and operational measures. Thus, preventive response and emergency response are allowed. Topology reconfiguration and generator redispatch are employed in both pre-event and post-event state. Load curtailment is only allowed in emergency response since the normal operation condition need to be maintained in preventive state.

Chapter 3 Research Methodology

To cope with the severe windstorms around the world, a two-stage integrated response framework is proposed in section 1. The framework is used to provide suggestion to distribution system operators about the integrated response measures against windstorms. The example of fragility curves and the method of failure probability calculation of lines and towers are presented in section 2. Based on the introduction in section 2, the outline of the two-stage scenario-based stochastic model is shown in section 3. The progressive hedging algorithm is finally presented in section 4 as a solving methodology to the stochastic problem.

3.1 Two-stage Integrated Response Framework
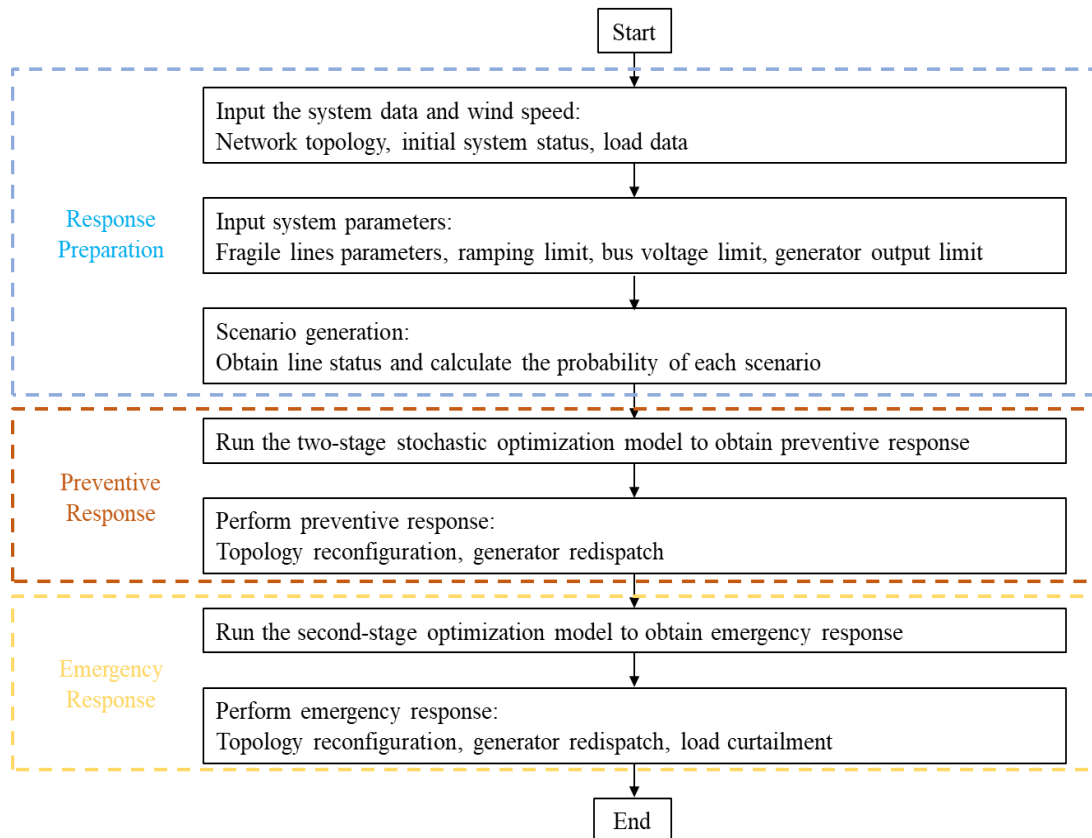
Figure 3.1 Two-stage integrated response framework.

Figure 3.1 is a two-stage integrated response framework to deal with the up-coming windstorms. Distribution system operators get advice on how to perform the response before and after the event by employing the framework. Response preparation, preventive response and emergency response are the three steps in the integrated response framework. System data such as network topology, initial system status, and load data are obtained by situational awareness. It is assumed that situational awareness is sufficient in the thesis. System parameters include fragile lines parameters, ramping limit of distributed energies, bus voltage limit and generator output limit. These parameters are essential in model constraints and make impact on the effectiveness of improvement measures.

In the next step, system operators run the two-stage optimization model to obtain optimal preventive response. The model considers all the possible scenarios and the calculation of scenario probability is expressed in the next section. The preventive response provides distribution operators a possible way to deal with the up-coming extreme weather event. System operators performs the preventive response including topology reconfiguration and generator redispatch. The event comes after the preventive response is employed and causes damage to system component as distribution lines and tower. Notice that the component status is determined by the actual damage of event and is fixed once the event occurs. Finally, the emergency response is obtained by running the second-stage optimization model. The detailed interpretation of the relationship between two models is given in section 3.

3.2 Fragility Curve and Failure Probability

To obtain the optimized distribution system topology reconfiguration under natural disasters, the uncertainty of component failure towards an event must be considered. The main component in the thesis is distribution lines and towers and the failure rate of distribution lines is regarded as the function of wind speed. To map the component failure rate with wind speed, a fragility model of distribution lines [40] is introduced to simulate line status under different weather conditions.
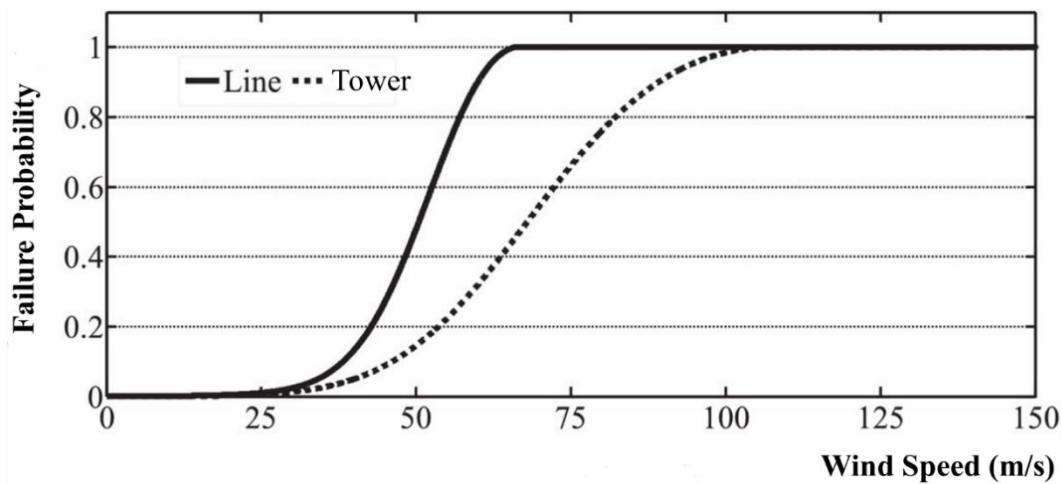
Figure 3.2 Typical fragility curve for distribution lines and towers [42].

Figure 3.2 is a typical distribution lines and tower fragility curve towards different wind speed. For both distribution lines and towers, each wind speed corresponds to a specific component failure probability. For instance, line failure probability is 0.4 under 50m/s wind speed. Tower failure probability is 0.8 when the wind speed reaches 60m/s. It means that once the wind speed is determined, the component failure probability can be obtained from these two figures. It is obvious and reasonable that towers are robust than lines with respect to a same wind speed and the threshold wind speed of definitely failure for towers is much higher than that of lines.

26

It is worth mentioning that **Figure 3.2** is the failure probability of one single component (line and tower), because a line is damaged if one of the components between two buses are damaged including towers and lines. The failure probability of branch b is calculated as follows:

$$P_b(w) = P_{b,B}(w) + P_{b,T}(w) - P_{b,B}(w)P_{b,T}(w) \tag{3.1}$$

where $P_b(w)$ is the failure probability of branch b when the wind speed is w. $P_{b,B}(w)$ and $P_{b,T}(w)$ are failure probabilities of branch b because of conductor and pole damage. $P_{b,B}(w)$ is from the line fragility curve in **Figure 3.1(a)**.

Suppose the failure of distribution towers is an independent event and each tower are in the same weather condition, $P_{b,T}(w)$ is expressed as:

$$P_{b,T}(w) = 1 - (1 - P_T(w))^{N_T} \tag{3.2}$$

where $P_T(w)$ is the single tower failure probability under wind speed w, which is obtained from **Figure 3.1(b)**, and N_T is number of towers in branch b.

The uncertainty in component failure comes from the uncertainty of windstorm impact to power system. Under this circumstance, there are many possible "scenarios" after one specific windstorm occurs. Here "scenario" means possible line status or possible lines status profile when there is more than one fragile line in the system. For a distribution system with only one fragile line, two possible scenarios are considered. The line failure probability is $P_b(w)$, while the survive probability is $1 - P_b(w)$. **Table 3.1** is the list of all scenarios and probabilities for a system with two fragile lines. Assume that the failure probability of these two fragile lines are $P_{b,1}(w)$ and $P_{b,2}(w)$.

Table 3.1 Scenarios and probabilities for a two fragile lines system.

Status of line 1	Status of line 2	Probability of the scenario
In service	In service	$(1- P_{b,1}(w)) (1- P_{b,2}(w))$
In service	Out of service	$(1- P_{b,1}(w)) P_{b,2}(w)$
Out of service	In service	$P_{b,1}(w) (1- P_{b,2}(w))$
Out of service	Out of service	$P_{b,1}(w) P_{b,2}(w)$

For a system with N fragile lines, there are 2^N scenarios in total. The scenario probability is given:

$$P_s(w) = \prod_{1}^{N_1} P_{b,n}(w) \prod_{N_1}^{2^N} (1 - P_{b,n}(w)) \tag{3.3}$$

where $P_s(w)$ is scenario probability and $P_{b,n}(w)$ is the damage probability of nth fragile line in wind speed w. Line 1 to line N_1 are assumed to be destroyed by windstorms while line N_1+1 to line 2^N are survived.

Since the main purpose of this thesis is to obtain the optimized integration of preventive and emergency responses to enhance distribution system resilience, wind speed is predetermined and no uncertainty is considered in weather severity.

3.3 Scenario-based Model

Based on the proposed integrated response framework in section 1 and scenario probability calculation in section 2, the key of the framework is formulated as a two-stage stochastic problem. The overall objective function is to minimize the expected total cost in the process of integrated response. Due to the uncertainty of line damage status after windstorms, the second stage problem is probabilistic and all the possible scenarios are considered. The scenario-based model is expressed as:

$$\min \quad C_1 + \sum_{S} C_{2(s)} P_s \tag{3.4}$$

where C_1 refers to the cost of preventive response in the first stage, while $C_{2(s)}$ is the cost of emergency response in the second stage correspond to scenario s. P_s is the probability that scenario s occurs and is calculated by formula (3.3). According to the definition of expected value, the expected emergency cost is the sum of the product of cost $C_{2(s)}$ and probability P_s in each scenario. The preventive stage cost is mainly the reconfiguration cost and the emergency response cost is consist of reconfiguration cost and load shedding cost.

To be specific, denote X as the first-stage variables, and Y_s as the second-stage decisions variables to scenario, formula (3.4) is rewritten as:

$$\min \quad cX + \sum_{S} F_2(Y_s) P_s \tag{3.5}$$

It is obvious that:

$$\begin{cases} C_1 = cX \\ C_{2(s)} = F_2(Y_s) \end{cases} \tag{3.6}$$

The two-stage constraints are given as:

$$\begin{cases} AX \le b \\ DY_s \le e \end{cases}, \forall s \in S \tag{3.7}$$

where $AX \le b$ represents the first-stage constraints. $DY_s \le e$ is the second-stage constraints. Power balance constraints, generator ramping and output limits exist in both two stages.

Formula (3.5) and (3.7) is the scenario-based stochastic model in the integrated response framework. Distribution system operators run the model before event to obtain the preventive response and perform it. Once the event comes, the component damage status is determined by the actual situation, which means that the scenario is fixed. Then

the second-stage optimization is performed to get the emergency response, which is expressed as:

$$\min \ F_2(\boldsymbol{Y}_{s.real}) \tag{3.8}$$

$$D\boldsymbol{Y}_{s,real} \leq e \tag{3.9}$$

where $\boldsymbol{Y}_{sreal}$ refers to the decision variables after events including topology reconfiguration, generator output and bus load shedding. Since the preventive response has been performed and the line damage status is determined at that time, the first-stage decision variables do not exist in the objective function of second model. And the constraints of second model are absolutely identical to the second-stage constraints in the previous two-stage model, which illustrates the relationship between two-stage model and second-stage model.

3.4 Introduction of Progressive Hedging Algorithm
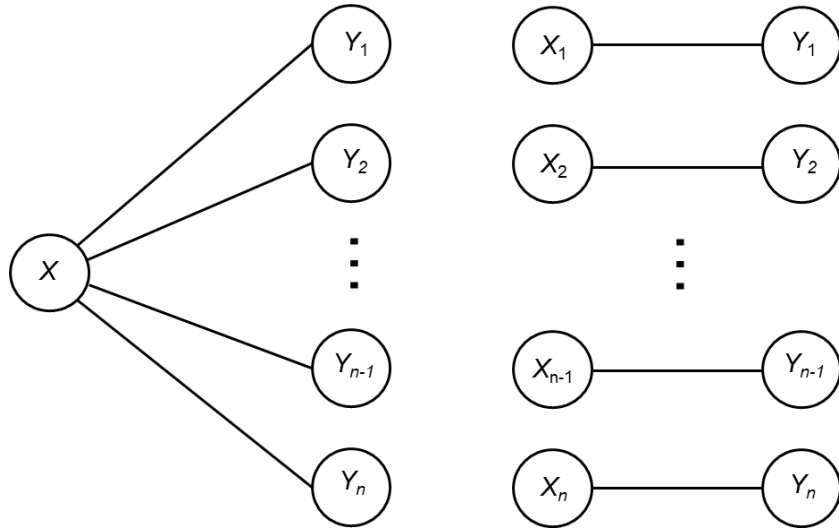
Figure 3.3 Comparison of the initial two-stage problem and PH algorithm.

Different scenario decomposition techniques are employed when faced with scenario-based model in resilience improvement problem. Benders' decomposition is commonly used in scenario-based problem. However, Benders' decomposition

performs poorly in such problems because of the heavy computation burden. Since the problem is modeled as a two-stage stochastic formulation with binary variables. In that situation, progressive hedging (PH) algorithm take into position in several scenario-based resilience improvement problem and performs well [37][51][52].

The two-stage structure plays a role in Bender's decomposition in two-stage optimization, while the PH algorithm integrates the two stages. In PH algorithm, the original two-stage problem is decomposed into many scenarios. Each scenario has one first-stage solution and they may differ for different scenario. Since the optimized first-stage decisions differ in each scenario, a penalty coefficient is added to the decision to get the convergence. When the optimization gap converges within an acceptable range, the first-stage in that iteration is regarded as the final solution. To give a clear explanation of PH decomposition, **Figure 3.3** is a comparison of the initial two-stage problem and PH algorithm.

The scenario-based PH algorithm proves to be an effective method to deal with two-stage stochastic models associated with integers. It is reasonable to be employed in this integration measures problem. The detail procedure of PH algorithm for a two-stage stochastic problem is shown below [56].

For a two-stage optimization problem (3.6), the steps of PH algorithm are shown in follows. $\rho > 0$ is a penalty factor and ϵ is termination criteria or convergence gap. Many researches have been devoted to compute effective ρ values and the best ρ is expressed as:

$$\rho = \frac{c}{X_{max} - X_{min} + 1} \tag{3.10}$$

c is the first-stage decision variables cost. In this thesis, it represents the unit cost of topology reconfiguration.

1. k=0

2. For all $s \in S, X_s^{(k)} = argmin_x(cX + F_2(Y_s))$

3. $\bar{X}^{(k)} = \sum_{s \in S} P_s X_s^{(k)}$

4. $\omega_s^{(k)} = \rho(X_s^{(k)} - \bar{X}^{(k)})$

5. $k = k + 1$

6. For all $s \in S, X_s^{(k)} = argmin_x(cX + \omega_s^{(k-1)}X + \rho/2\|X - \bar{X}^{(k-1)}\|^2 F_2(Y_s))$

7. $\bar{X}^{(k)} = \sum_{s \in S} P_s X_s^{(k)}$

8. For all $s \in S, \omega_s^{(k)} = \omega_s^{(k-1)} + \rho(X_s^{(k)} - \bar{X}^{(k)})$

9. $g^{(k)} = \sum_{s \in S} P_s \|X_s^{(k)} - \bar{X}^{(k)}\|$

10. If $g^{(k)} < \epsilon$, then go to step 5. Otherwise, terminate.

Chapter 4 Optimization Model

A two-stage stochastic problem is presented to obtain preventive and emergency response measures to improve distribution system in this chapter. The objective function is presented and constraints are listed in section 2 including first-stage constraints and second-stage constraints. The first stage is to do the preventive measures including topology reconfiguration and generator dispatch, while the emergency measures involves topology reconfiguration, generator redispatch and load curtailment. Section 3 gives detail interpretation of the essential formulations in the model, while section 4 shows the linearization procedure for the nonlinear constraints. The solving method, PH algorithm, is illustrated in section 5.

4.1 Objective Function

$$min(\sum_{(i,j)\in SL} \left| y_{i,j}^a - y_{i,j}^0 \right| c_{i,j}^a + \sum_{s\in S} \omega_s \Omega(s)) \tag{4.1}$$

where

$$\Omega(s) = \min(c_{shed} \sum_{i\in DB} P_{shed}^{c,s} \Delta t + \sum_{(i,j)\in SL} \left| y_{i,j}^c - y_{i,j}^a y_{i,j}^b \right| c_{i,j}^c) \tag{4.2}$$

In this objective function, the target is to minimize switching cost in preventive response plus expected emergency response cost which include load curtailment cost and switching cost considering all possible scenarios. (4.1) and (4.2) show the first-stage and second-stage objective functions. The calculation of second stage cost also involves an optimization problem.

4.2 Constraints

4.2.1 First-stage Constraints

$$\sum_{g \in G_i} P_g^a - \sum_{(i,j) \in L_i} y_{i,j}^a P_{i,j}^a = \sum_{d \in D_i} P_d, i \in B \tag{4.3}$$

$$\sum_{g \in G_i} Q_g^a - \sum_{(i,j) \in L_i} y_{i,j}^a Q_{i,j}^a = \sum_{d \in D_i} Q_d, i \in B \tag{4.4}$$

$$P_{i,j}^a = G_{i,j}\left(V_{i,j}^{a\,2} - V_i^a V_j^a \cos\theta_{i,j}^a\right) - B_{i,j} V_i^a V_j^a \sin\theta_{i,j}^a, (i,j) \in L \tag{4.5}$$

$$Q_{i,j}^a = -B_{i,j}\left(V_{i,j}^{a\,2} - V_i^a V_j^a \cos\theta_{i,j}^a\right) - G_{i,j} V_i^a V_j^a \sin\theta_{i,j}^a, (i,j) \in L \tag{4.6}$$

$$-y_{i,j}^a P_{i,j}^{max} \le P_{i,j}^a \le y_{i,j}^a P_{i,j}^{max}, (i,j) \in L \tag{4.7}$$

$$P_g^{min} \le P_g^a \le P_g^{max}, g \in G \tag{4.8}$$

$$V_i^{min} \le V_i^a \le V_i^{max} \tag{4.9}$$

$$\sum_{(i,j) \in L} y_{i,j}^0 (1 - y_{i,j}^a) \le K_I^a \tag{4.10}$$

$$\sum_{(i,j) \in L} (1 - y_{i,j}^0) y_{i,j}^a \le K_O^a \tag{4.11}$$

$$\sum_{(i,j) \in L} y_{i,j}^a = n - 1 \tag{4.12}$$

$$\beta_{i,j}^a + \beta_{j,i}^a = y_{i,j}^a, (i,j) \in L \tag{4.13}$$

$$\sum_{j \in B} \beta_{i,j}^a = 1, i = 1,2,\dots,n \tag{4.14}$$

$$\beta_{1,j}^a = 0, j \in GB \tag{4.15}$$

The first-stage constraints of distribution systems are represented by (4.3)-(4.15).

Constraints (4.3)-(4.6) ensure load balance for each bus and branch in distribution

34

system after preventive response. $P^a{}_g$ and $Q^a{}_g$ represent the generator output. $V^a{}_{i,j}$ and $\theta^a{}_{i,j}$ represent the magnitude and angle of each bus voltage. Constraints (4.7)-(4.9) show the boundary of generator output, branch power flow and bus voltage magnitude. The superscript "max" means the upper boundary of those variables, while the subscript "min" means the lower boundary of variables. Constraints (4.10) and (4.11) indicate that the number of in-service-lines that we can cut off and the number of off-service lines that we can closed are limited in the preventive response, which are represented by $K^a{}_I$ and $K^a{}_O$.

Constraints (4.12)-(4.15) ensure that the distribution system operating in radial mode, not in loop mode. It is because that when distribution system operating in loop mode, there are loop current which may influence the normal operation of distribution system. Constraints (4.12) indicates that whatever the preventive reconfiguration is, the number of on-service-lines is one less than the bus number. $\beta_{i,j}=1$ if i is the parent bus of j, vice versa. Constraints (4.14) ensures that one bus is corresponding to one parent bus except original bus. Constraints (4.15) indicates that those buses with generator can't have parent bus.

4.2.2 Second-stage Constraints

$$\sum_{g\in G_i} P_g^{c,s} - \sum_{(i,j)\in L_i} y_{i,j}^{c,s} P_{i,j}^{c,s} + \sum_{d\in D_i} P_{shed}^{c,s} = \sum_{d\in D_i} P_d , i \in B \qquad (4.16)$$

$$\sum_{g\in G_i} Q_g^{c,s} - \sum_{(i,j)\in L_i} y_{i,j}^{c,s} Q_{i,j}^{c,s} + \sum_{d\in D_i} Q_{shed}^{c,s} = \sum_{d\in D_i} Q_d , i \in B \qquad (4.17)$$

$$P_{i,j}^{c,s} = G_{i,j} \left(V_{i,j}^{c,s\,2} - V_i^{c,s} V_j^{c,s} \cos\theta_{i,j}^{c,s} \right) - B_{i,j} V_i^{c,s} V_j^{c,s} \sin\theta_{i,j}^{c,s}, (i,j) \in L \qquad (4.18)$$

$$Q_{i,j}^{c,s} = -B_{i,j}\left(V_{i,j}^{c,s\,2} - V_i^{c,s}V_j^{c,s}\cos\theta_{i,j}^{c,s}\right) - G_{i,j}V_i^{c,s}V_j^{c,s}\sin\theta_{i,j}^{c,s}, (i,j) \in L \quad (4.19)$$

$$-y_{i,j}^{c,s}P_{i,j}^{max} \le P_{i,j}^{c,s} \le y_{i,j}^{c,s}P_{i,j}^{max}, (i,j) \in L \quad (4.20)$$

$$P_g^{min} \le P_g^a \le P_g^{max}, g \in G \quad (4.21)$$

$$V_i^{min} \le V_i^a \le V_i^{max} \quad (4.22)$$

$$P_g^{c,s} - P_g^a \le P_g^{rp.max}\Delta t, g \in G \quad (4.23)$$

$$y_{i,j}^{c,s} \le y_{i,j}^b, (i,j) \in L \quad (4.24)$$

$$\sum_{(i,j)\in L} y_{i,j}^a y_{i,j}^b (1 - y_{i,j}^c) \le K_I^c \quad (4.25)$$

$$\sum_{(i,j)\in L} (1 - y_{i,j}^a) y_{i,j}^b y_{i,j}^c \le K_O^c \quad (4.26)$$

The second-stage constraints of distribution systems are represented by (4.16)-(4.26), which are very similar to the first-stage constraints. Notice that second-stage constraints are applicable to each scenario. Constraint (4.16)-(4.19) ensure load balance for each bus and branch in distribution system after emergency response. Constraints (4.20)-(4.22) show the boundary of generator output, branch power flow and bus voltage magnitude. Constraint (4.23) shows the ramping limit of generator because of the short duration of emergency response. Constraint (4.24) indicate that damaged lines cannot be closed in the emergency response since it is already destroyed. Constraints (4.25) and (4.26) indicate that the number of in-service-lines that we can cut off is still limited in the emergency response, so as the number of off-service-lines that we can closed, which are represented by $K^{c,s}{}_I$ and $K^{c,s}{}_O$.

4.3 Interpretation of the Model

The objective function in this model is to find best preventive topology reconfiguration $y^a_{i,j}$ to minimize the total cost considering all possible consequence of a specific windstorm. As is mentioned before, the model is formulated as a two-stage problem. The first-stage cost is fixed once the preventive measures is employed, while the second stage cost are still uncertain and will be influenced by the possible damage status of system component.

The first stage cost, topology switching cost, is expressed as $|y^a_{i,j} - y^0_{i,j}|c^a_{i,j}$. In the emergency response, load shedding cost and topology switching cost are included. They both depend on the specific scenario, in which the damage status of a line is a random variable. In probability theory, the expected value X of a random variable with consequences x_1, x_2, …, x_k and corresponding probabilities p_1, p_2, …, p_k is:

$$\mathrm{E}[X] = \sum_{i=1}^{k} x_1 p_1 + x_2 p_2 + \cdots + x_k p_k \qquad (4.27)$$

Let Ω_s be the outcome and P_s be the probability, the expected cost of second stage is expressed as:

$$\sum_{s \in S} \omega_s \Omega(s) \qquad (4.28)$$

where the randomness comes from the uncertainty of the component damage status under windstorms. The probability ω_s of scenario s is calculated by formula (3.3) and the outcome Ω_s includes load shedding cost and topology switching cost.

Generally, the first-stage constraints and second-stage constraints share many similarities and in same formulation. Power balance constraints, generator output limit

and number of switching limit exist in both preventive response and emergency response. The main differences lay in the radial constraints in the first stage and the ramp rate constraints and the topology reconfiguration constraints in the second stage.

Ramping rate constraint (4.23) is essential for load balance in the post-event state. As is mentioned before, the time period we focused on ends when the emergency measures are fully employed, which is set as an hour. The main grid power availability and distributed energy ramp constraint make impact on the power balance and the amount of load curtailment in the second stage, then load shedding cost. Besides, due to the short time duration of emergency responses, the damaged components are remained unrepaired in emergency measures. As constraint (4.24) shows, they can't be switched on. Radial constraints appear only in the first-stage constraints. The radial system is simple and the least expensive, which can be easily expanded by the inclusion of additional transformers. However, the radial constraints may not hold after event because of the lacking of energy and equipment resources.

4.4 Linearization

The proposed two-stage stochastic program forms a linear model excepting objective function (4.1) (4.2) and first-stage constraints (4.5) (4.6). Second stage constraints (4.18) and (4.19) can be linearized by the same method as that in first-stage constraints since they share the same formulation. (4.25) and (4.26) also need to be linearized since they contain the multiproduct of binary variables.

Absolute value in objective function (4.1) is easily eliminated by assuming that the initial system line status is predetermined. All no-tie branches are closed while all

tie branches are not. Then the topology switching occurs only if no-tie branches are switched off or tie branches are switched on. Objective function is rewritten as:

$$\min(\sum_{(i,j)\epsilon SL_{tie}} (y_{i,j}^a - y_{i,j}^0)c_{i,j}^a + \sum_{(i,j)\epsilon SL_{no-tie}} (y_{i,j}^0 - y_{i,j}^a)c_{i,j}^a + \sum_{s\in S} \omega_s \Omega(s) \quad (4.29)$$

where initial system line status $y^0{}_{i,j}$ is known. The only decision variables are preventive topology reconfiguration $y^a{}_{i,j}$, making the objective function linear.

Objective function (4.2) is equivalent to the flowing formulation with three additional constraints:

$$\Omega(s) = \min(c_{shed} \sum_{i\in DB} P_{shed}^{c,s} \Delta t + \sum_{(i,j)\in SL} M_{i,j} c_{i,j}^c) \quad (4.30)$$

$$y_{i,j}^c - y_{i,j}^c y_{i,j}^b \leq M_{i,j}, (i,j) \in L \quad (4.31)$$

$$y_{i,j}^c - y_{i,j}^c y_{i,j}^b \geq -M_{i,j}, (i,j) \in L \quad (4.32)$$

$$M_{i,j} \geq 0 \quad (4.33)$$

Equations (4.5) and (4.6) are approximated as [57] follows and θ is bus voltage angle:

$$P_{i,j}^a = G_{i,j}(V_i - V_j - r_{(i,j)} + 1) - B_{i,j}(\theta_i - \theta_j) \quad (4.34)$$

$$Q_{i,j}^a = -B_{i,j}(V_i - V_j - r_{(i,j)} + 1) - G_{i,j}(\theta_i - \theta_j) \quad (4.35)$$

where $r_{(i,j)}$ represents the linear approximation of $\cos\theta_{i,j}$ which could also be wrote as follow formula:

$$r_{(i,j)} = d_{(i,j),u}(\theta_i - \theta_j) + e_{(i,j),u} \quad (4.36)$$

To deal with quadratic terms and cubic terms in (4.25) and (4.26), three binary variables are introduced, $y_{i,j,1}= y^a{}_{i,j} y^b{}_{i,j}$, $y_{i,j,2}= y^b{}_{i,j} y^c{}_{i,j}$ and $y_{i,j,3}= y^a{}_{i,j} y^b{}_{i,j} y^c{}_{i,j}$, then (4.25) and (4.26) become:

$$\sum_{(i,j)\in L} (y_{i,j,1} - y_{i,j,1}) \le K_I^c \tag{4.37}$$

$$\sum_{(i,j)\in L} (y_{i,j,2} - y_{i,j,3}) \le K_O^c \tag{4.38}$$

where $y_{i,j,1}$, $y_{i,j,2}$ and $y_{i,j,3}$ are the products of several binary variables, which is calculated by following formula:

$$y = \prod_{k\in\mathcal{N}} y_k \Leftrightarrow \begin{cases} y \le y_k, k \in \mathcal{N} \\ y \ge \sum_{k\in\mathcal{N}} y_k - num(\mathcal{N}) + 1 \end{cases} \tag{4.39}$$

where $num(\cdot)$ is the elements number in set N, and y_k and y are binary variables.

In conclusion, the objective function of rewritten model is formula (4.29) and (4.30), while the constraints are (4.3), (4.4), (4.7)-(4.17), (4.20)-(4.26), (4.31)-(4.39).

4.5 Progress Hedging Algorithm in the Model

To make the discussion easier, a compact notation of proposed model is written as follows.

$$\min \quad \boldsymbol{c}^{\mathrm{T}}(\boldsymbol{x} - \boldsymbol{x_0}) + \sum_{s\in S} \omega_s\, \varOmega(\boldsymbol{x}, s) \tag{4.40}$$

$$\text{s.t. } \boldsymbol{Ax} \le \boldsymbol{b} \tag{4.41}$$

$\boldsymbol{x}$ is the topology reconfiguration in preventive response and $\boldsymbol{x_0}$ is the initial line status. Vector $\boldsymbol{c}$ is the unit cost of topology switching. Constraint (4.41) corresponds to the first-stage constraints in the previous model. $\varOmega(\boldsymbol{x},s)$ is the second-stage emergency response problem for scenario s, which can be formulated in:

$$\varOmega(\boldsymbol{x}, s) = \min \quad \boldsymbol{g}(s)^{\mathrm{T}}\boldsymbol{y}(s) \tag{4.42}$$

$$\text{s.t. } \boldsymbol{Fy}(s) \le \boldsymbol{r}(s) - \boldsymbol{e}(s)\boldsymbol{x} \tag{4.43}$$

where $y(s)$ is the topology reconfiguration in emergency response for scenario s and the second-stage constraints are represented by (4.43). $g(s)$ is the unit topology switching cost and unit load shedding cost.

Let $(x, y(s)) \in K(s)$ represents two stage constraints (4.41) and (4.43), the simplified-express model can be formulated as follows:

$$z = \min \left\{ c^{\mathrm{T}}(x - x_0) + \sum_{s \in S} \omega_s \, g(s)^{\mathrm{T}} y(s), (x, y(s)) \in K(s), s \in S \right\} \quad (4.44)$$

1. Let $k=0$ and $m(s)^k=0, s=1, 2, \ldots, S$. For each s, compute:

$(x(s)^{k+1}, y(s)^{k+1})=\operatorname{argmin}\{c^{\mathrm{T}} x(s)+ g(s)^{\mathrm{T}} y(s), (x(s), y(s)) \in K(s)\}$.

2. $k= k+1$.

3. $x_{\mathrm{ave}}{}^k=\sum_{s \in S} P(s) \, x(s)^k$.

4. $m(s)^k = m(s)^{k-1}+\rho(x(s)^k- x_{\mathrm{ave}}{}^k), s=1, 2, \ldots, S$.

5. For each s, compute:

$(x(s)^k, y(s)^k)=\operatorname{argmin}\{c^{\mathrm{T}} x(s)+ g(s)^{\mathrm{T}} y(s)+ m(s)^k x(s)+\rho \|x(s)- x_{\mathrm{ave}}{}^k\|^2,$

$(x(s), y(s)) \in K(s)\}$.

6. Compute $d(k)=\sum_{s \in S} P(s) \| x(s)^k- x_{\mathrm{ave}}{}^k \|$. If $d(k) \leq \delta$, terminate. If not, go to Step 2.

Figure 4.1 Steps of PH algorithm

The detailed PH algorithm for this two-stage model is shown in **Figure 3.4**. Step 1 is used to obtain the first-time solution of each scenario. In each iteration, the expected value $x_{\mathrm{ave}}{}^k$ is calculated using the probability and the solution of each scenario. And the item $m(s)^k$ are calculated in Step 4, which are further used in updating objective function in Step 5. Two penalty items are added in Step 5 to obtain the updated solution for each

41

scenario. The deviation of $d(k)$ is expressed in Step 5 to test the termination criteria, where $d(k)$ denotes the expected deviation between solution $x(s)^k$ for each scenario and expected value x_{ave}^k in k^{th} iteration.

Chapter 5 Case Study

This chapter does two case studies in IEEE 33 bus system and a modified 69 bus system to illustrate the correctness and effectiveness of proposed framework and model. The results show that employing the integrated response helps to improve distribution resilience, meanwhile the cost is minimized for both connected system and isolated system. Besides, parameter sensitivity analysis is developed in both cases. Finally, the case study conclusion is presented in section 3.

5.1 Case Study in IEEE 33 Bus System

5.1.1 System data and Parameters

In this case study, IEEE 33 bus system is used to check the efficacy of the method and model. The system is set to connect to the bulk power system and bulk power system can provide power resources and ramping ability to distribution system. The initial topology of IEEE 33 bus system is shown in **Appendix A** [58]. The total load is 3.715 MW and the maximum power main grid provide is set as equal to the total load. The base power is S_{base}=100MW and base voltage is V_{base}=12.66kV. The upper and lower boundary of bus voltage magnitude are set as 1.05 and 0.95, respectively.

To eliminate the absolute value in objective function, all the five tie-branches are open at the initial state, when all the no-tie-branches are closed to guarantee the system normal operation. It is reasonable to assume that not all the branches are equipped with breakers. Assuming all tie-branches are with breakers and four no-tie-branches are with breakers, 6-7, 7-8, 9-10, 10-11. Seven distributed energies are attached on the system to maintain the bus voltage and related data is given in **Table 5.1**. The ramping limits

in preventive state and emergency state are set as 0.007MW and 0.003 MW respectively. To simplify the problem, these DGs are assumed to totally dispatchable and are not influenced by natural disasters. The unit load shedding cost is 10$/kWh. The preventive reconfiguration unit cost is $200 and $300 for no-tie-branches and tie-branches, respectively, while $400 and $1000 for no-tie-branches and tie-branches in emergency response since the lack of resources after windstorms.

Table 5.1 DG locations and output limits.

DG Number	DG Location	P_{max} (MW)	P_{min} (MW)	Q_{max} (MW)	Q_{min} (MW)
1	Bus 3	0.2	0.02	0.16	-0.16
2	Bus 4	0.15	0.015	0.16	-0.16
3	Bus 9	0.2	0.02	0.16	-0.16
4	Bus 13	0.2	0.02	0.16	-0.16
5	Bus 17	0.2	0.02	0.16	-0.16
6	Bus 29	0.2	0.02	0.16	-0.16
7	Bus 32	0.15	0.015	0.16	-0.16

Figure 5.1 shows the relationship between component failure probability and wind speed [59]. In this case study wind speed is set as 45m/s and no weather forecast deviation is considered in the thesis. The single line failure probability is 0.3 and tower is 0.1. Branch 2-3, 5-6, 7-8, 10-11 are fragile lines and their failure probability is calculated by formula (3.1) and (3.2), while other lines are assumed to be strong enough to withstand the up-coming windstorms.

The case study is programmed in Matlab 2018a and solved by CPLEX 12.4.
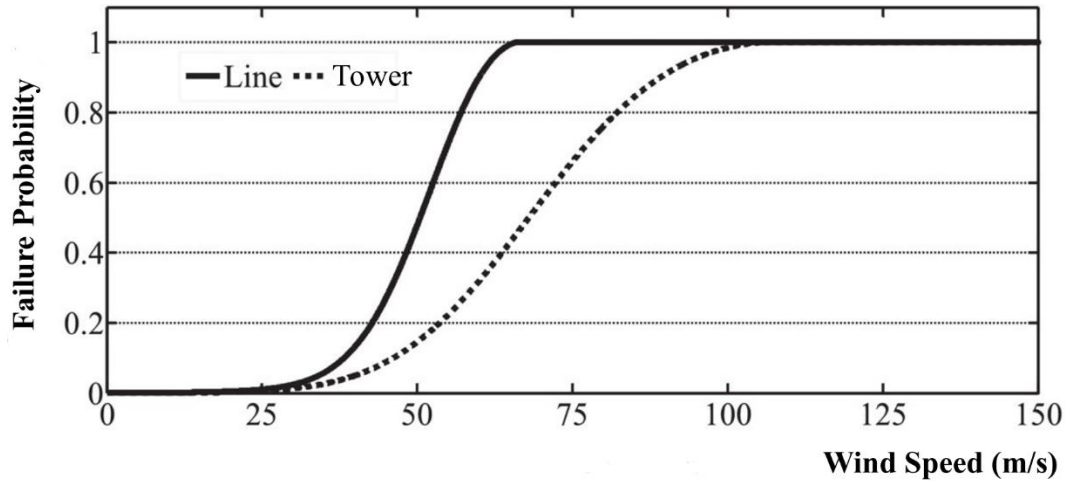
Figure 5.1 Component failure probability curve in distribution system.

5.1.2 Scenario Generation

Based on the component failure probability under wind speed 45m/s and formula (3.1) and (3.2), 16 scenarios are developed for 4 fragile lines and the scenario probability is shown in follow **Table 5.2**. Notice that the sum of all scenario probability is 1.

Table 5.2 Line status and probability for all scenarios.

Scenario	Line 2-3 Status	Line 5-6 Status	Line 7-8 Status	Line 10-11 Status	Scenario Probability
1	0	0	0	0	0.0978
2	0	0	0	1	0.1281
3	0	0	1	0	0.0579
4	0	0	1	1	0.0759
5	0	1	0	0	0.0492
6	0	1	0	1	0.0645
7	0	1	1	0	0.0292
8	0	1	1	1	0.0382
9	1	0	0	0	0.0831
10	1	0	0	1	0.1088
11	1	0	1	0	0.0492
12	1	0	1	1	0.0644
13	1	1	0	0	0.0418
14	1	1	0	1	0.0548
15	1	1	1	0	0.0248
16	1	1	1	1	0.0324

5.1.3 Integrated Response Results
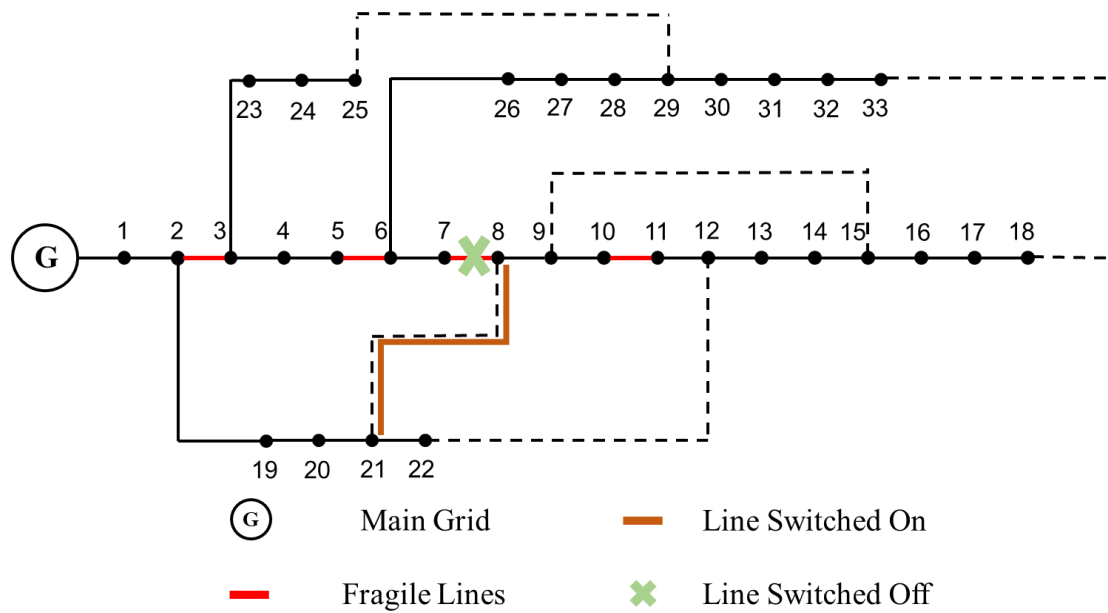
Figure 5.2 Illustration of topology reconfiguration in preventive response.
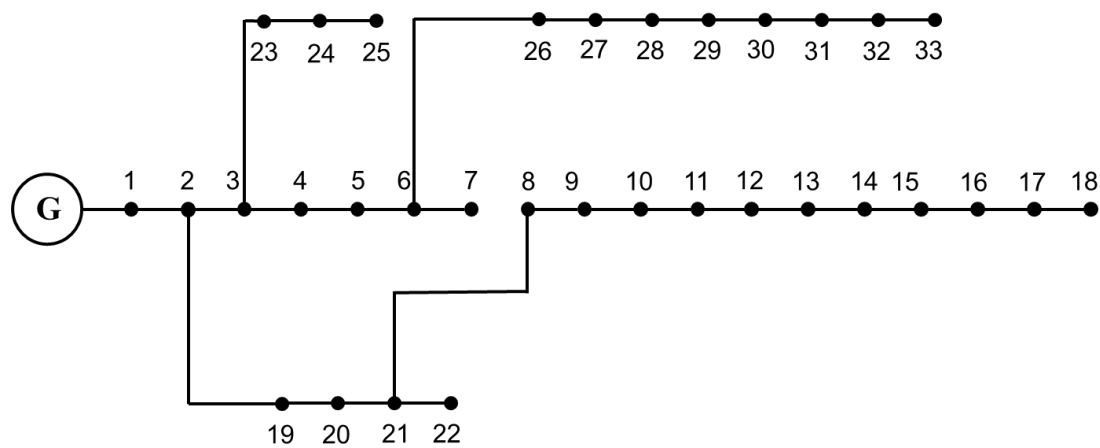
Figure 5.3 System topology after preventive response.

In this case study, preventive topology reconfiguration, emergency generator redispatch as emergency topology reconfiguration are allowed to maximize the benefit of integrated response. The computation time is 269s and the total cost is $10,070. The computation time is acceptable when it comes to an operational problem since the system operators get the extreme weather alert 24-72 hours in advance. **Figure 5.2** is an illustration of preventive response. There are four vulnerable lines in the system

which could be destroyed by windstorms with a certain probability correspond to the wind speed. Line 7-8 is open in preventive stage to cope with the possible damage caused by windstorms, while tie-branch 21-8 is closed to make the system operate in radial mode. The integrated response result is shown in **Figure 5.3** and is implemented in preventive state. The emergency response will be carried out according to the damage of windstorms. The result provides a guideline to the distribution system operators that the integrated response can be employed to deal with the up-coming extreme weather event.

5.1.4 Scenario Comparison

To explore the effectiveness of proposed two-stage integrated response framework, 5 scenarios are considered by the main three responses in the framework: preventive topology reconfiguration (*Pre-To*), emergency generator redispatch (*Em-Gr*) and emergency topology reconfiguration (*Em-To*). Notice that these scenarios are totally different from the scenarios in 3.2 and 3.3, which is caused by the uncertainty of weather impact to system component. The results of each scenarios are presented in **Table 5.3** (✓ means employed ✘ means not employed).

Table 5.3 Five scenarios and the responses allowed.

Scenario	*Pre-To*	*Em-Gr*	*Em-To*	Expected Total Cost ($)	*Pre-To* Result
1	✘	✘	✘	15,448	No allowed
2	✓	✘	✘	13,477	7-8 off, 21-8 on
3	✓	✓	✘	12,394	6-7 off, 21-8 on
4	✘	✓	✓	10,387	No allowed
5	✓	✓	✓	10,070	7-8 off, 21-8 on

All the three responses are allowed in the case study in the last section, which is actually scenario 5 in **Table 5.3**. The total cost is reduced dramatically from $15,448 to $10,070 by employing the proposed integrated response framework, in which all the responses are allowed. It is because that topology reconfiguration in both two stages and generator redispatch in emergency state can provide flexibility to distribution system to mitigate the impact of windstorms. When no response is allowed in scenario 1, there is only load shedding cost in total cost. Besides, the amount of load shedding in scenario 1 is 1.5548 MWh, while scenario 5 only has 0.9444 MWh load curtailment, which means that distribution system resilience is improved by integrated response in a minimum cost.

It is obvious that total cost decreases gradually from scenario 1 to scenario 5 and the maximum gap is between scenario 1 and scenario 5, where all responses are allowed. It is also concluded that the benefit of integrated response is larger than the individual preventive and emergency response, since the total cost in scenario 5 is smaller than that in other scenarios. To explore the composition of total cost in the five scenarios, a detailed analysis of total cost is shown in **Table 5.4**.

Table 5.4 Detailed expected total cost analysis.

Scenario	*Pre-To* Cost ($)	Expected Load shedding Cost ($)	Expected *Em-To* Cost ($)	Expected Total Cost ($)
1	0	15,448	0	15,448
2	500	12,977	0	13,477
3	500	11,894	0	12,394
4	0	9,444	943	10,387
5	500	9,444	126	10,070

Compared to scenario 1, preventive topology reconfiguration is allowed in scenario 2. One no-tie-branch is open and one tie-branch is closed so the preventive cost is $500, and the load shedding cost is reduced dramatically by doing so. Once generator ramping is allowed in scenario 3, the load shedding cost is reduced furtherly since more load is supplied by the distributed generators. Only emergency response is allowed in scenario 4, where the post-event topology reconfiguration plays a significant role in improving system resilience and reducing load shedding cost. Comparing scenario 4 and 5, the load shedding cost is the same, while the total cost is reduced by doing topology reconfiguration before events. It is concluded that integrated response can improve resilience most with minimum cost.

5.1.5 Sensitivity Analysis
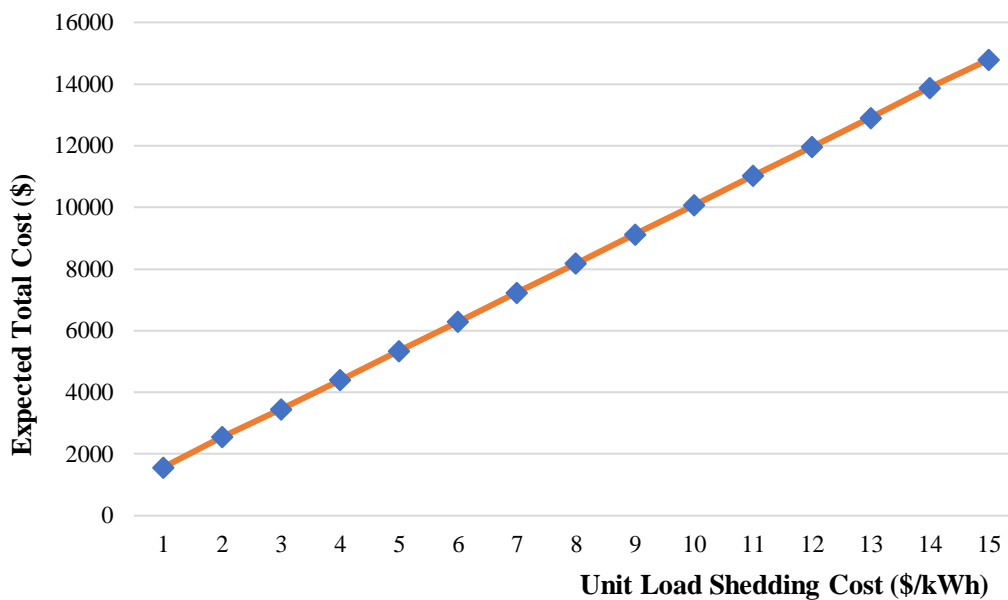
Figure 5.4 Expected total cost under different unit load shedding cost.

The comparison between different scenarios shows and effectiveness of the integrated response framework in distribution system resilience against windstorms.

The amount of load curtailment after event is reduced by applying preventive topology reconfiguration. The emergency response is deployed after the event since the damage status of system component is detected by situational awareness. Sensitivity analysis aims to investigate the influence of parameters to the solution and the total cost. Three parameters are put into sensitivity analysis.

It is obvious from **Table 5.4** that load shedding cost plays a significant role in total cost. It is reasonable to check the influence of unit load curtailment cost to the expected total cost, and the unit load curtailment cost is checked from 1$/kWh to 15$/kWh in 1$/kWh interval. As is shown in **Figure 5.4**, the total cost increases with the increasing of unit load shedding cost and the relationship between are regarded as linear. It is because in this case, the cost of distributed energy output is ignored and they produce the maximum output to reduce the load shedding. The reconfiguration cost under different unit load shedding cost is the same, and the only cost deviation comes from load shedding cost.

Table 5.5 Ramping limit sensitivity analysis.

Preventive Ramping Limit (MW/h)	Emergency Ramping Limit (MW/h)	Expected Total Cost ($)	Expected Load curtailment (MWh)
0.07	0.03	10,070	0.9444
0.06	0.03	10,266	0.9640
0.05	0.03	10,463	0.9837
0.04	0.03	10,698	1.0334
0.03	0.03	12,059	1.0223
0.03	0.04	10,660	1.0334
0.03	0.05	10,463	0.9837
0.03	0.06	10,266	0.9640
0.03	0.07	10,070	0.9440
0.03	0.08	10,070	0.9440

Table 5.5 is the ramping limit sensitivity analysis. The total cost and load shedding are tested under different preventive ramping limit and emergency ramping limit. The total cost and load shedding change in same direction. Either the change in preventive ramping limit or emergency ramping limit cause the change in total cost and load shedding. It can be seen that when emergency ramping limit exceeds 0.08MW/h, the result will not be changed since the distributed generators have already produced the maximum output and the relax in ramping limit make no influence on the generator output in emergency response.

As is mentioned before, wind speed determined by accurate weather forecast and is set as 45m/s in above study. Here the solutions in different wind speed are obtained to check the impact of the severity of windstorms to the total cost in resilience improvement. **Figure 5.5** and **Figure 5.6** are the expected load shedding and expected total cost of five scenarios with the change of wind speed. The first conclusion is that expected total cost and load shedding increases with the increase of wind speed since high wind speed increase the failure probability of system component. We can also see that the integrated response can produce more economic profit in resilience improvement than that in single preventive or emergency response. The total cost in single emergency response is less than that in preventive response. Besides, when the wind speed grows, the deviation between different scenarios decreases, which means that the effectiveness of resilience response decreases.

The expected total cost in scenario 3 is lower than that in scenario 4 under wind speed 55m/s, while the expected load shedding is still higher. It is caused by the failure

probability of fragile lines and scenarios. The preventive switching cost for scenario 3 is \$500 and scenario 4 is \$0 for all wind speed. The reduced expected load shedding cost under wind speed 55m/s is less than \$500. Thus, the expected total cost in scenario 3 is lower than that in scenario 4.
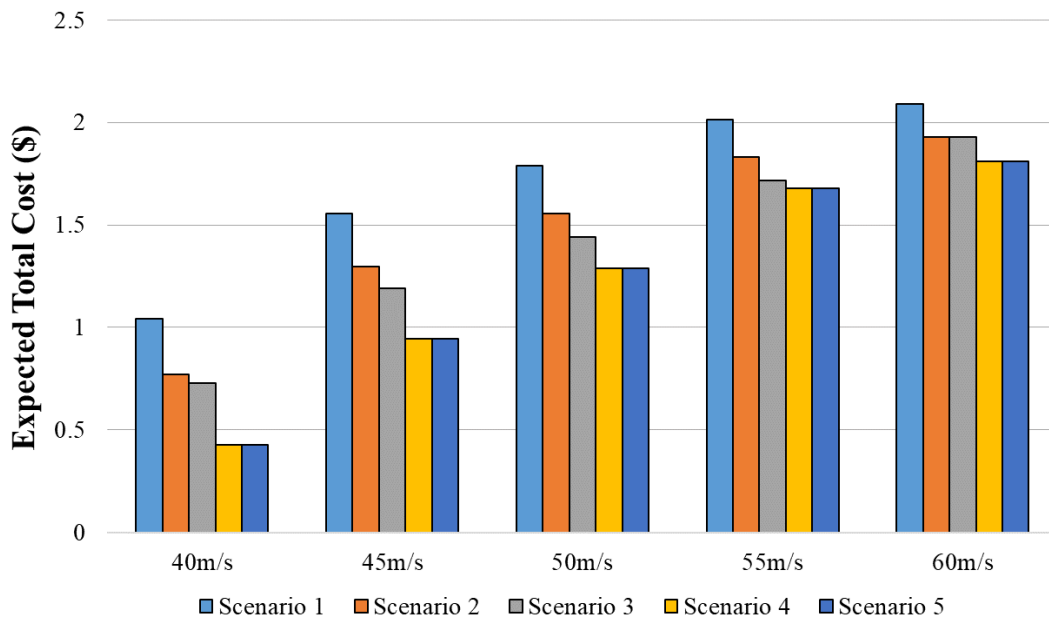
Figure 5.5 Expected load shedding of five scenarios under different wind speed.
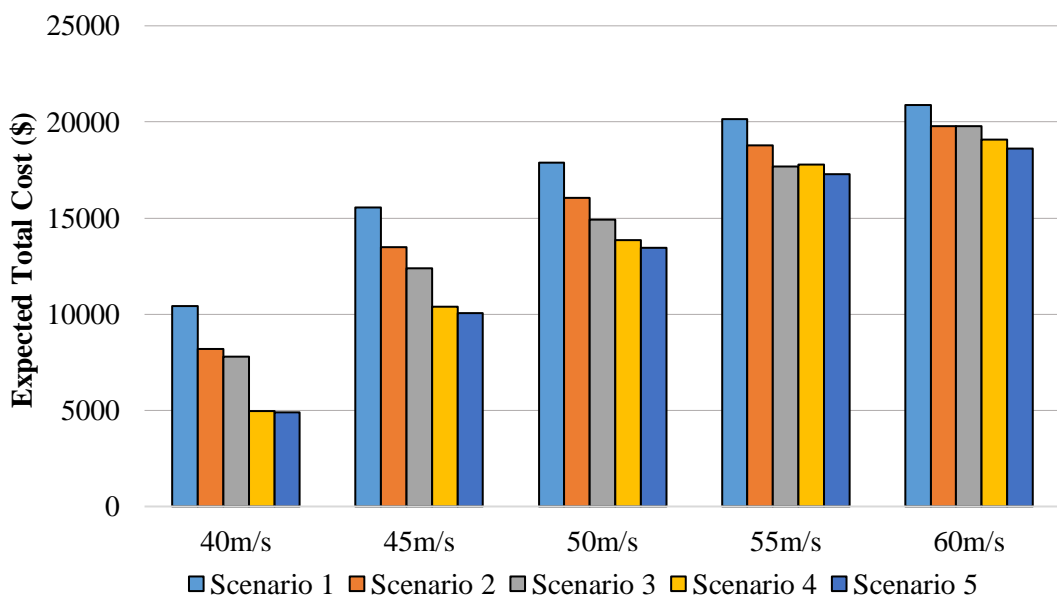
Figure 5.6 Expected total cost of five scenarios under different wind speed.

5.2 Case Study in Modified 69 Bus System

5.2.1 System Data and Scenario Generation

A modified 69 bus system is studied in this section. The system topology is shown in **Appendix C** and the system load and line data are in **Appendix D** [60]. To make the two systems comparable in total load, the bus load is reduced to three quarters and the total load is 4.039 MW. The base power is S_{base}=100MW and base voltage is V_{base}=11kV. The upper and lower boundary of bus voltage magnitude are set as 1.05 and 0.95, respectively. Different form the IEEE bus system which is attached to the bulk power system, the 69 bus system is assumed to operate in isolated mode, which means that the system obtains no power from power grid and all the power is provided by distributed energy attached in the system. The locations, ramping limits and output limits of DGs are shown in **Table 5.6**.

Table 5.6 DG locations, ramping and output limits.

DG Number	DG Location	P_{max} (MW)	P_{min} (MW)	Q_{max} (MW)	Q_{min} (MW)	Ramping Limit (MW/h)
1	Bus 4	1.2	0.12	1.2	0.12	0.25
2	Bus 9	1.0	0.10	1.0	0.10	0.53
3	Bus 17	1.3	0.13	1.3	0.13	0.25
4	Bus 39	0.6	0.06	0.6	0.06	0.25
5	Bus 47	0.7	0.07	0.7	0.07	0.25
6	Bus 55	0.7	0.07	0.7	0.07	0.25

To ensure the connectivity of initial system, tie-branch 1 and tie-branch 4 are set to closed at the initial state, while all the other tie-branches are open and all the no-tie-branches are closed guarantee the system normal operation. Similar to the previous study, only four lines are with breakers, 19-20, 23-24, 37-38 and 42-43. These

distributed generators are assumed to totally dispatchable and are not influenced by natural disasters. The unit load shedding cost and unit reconfiguration unit cost is total the same as previous study to make comparison.

Figure 5.1 is still used as fragility curves for modified 69 bus system. And the wind speed is set as 50m/s. Then the correspond single line failure probability and tower failure probability is 0.45 and 0.14. Calculated by formula (3.1) and (3.2), the fragile lines failure probability is in **Table 5.7** (assume that line resistance is 0.4Ω/km and the interval between two towers is 250m).

Table 5.7 Fragile line failure probability calculation.

Fragile Lines	Resistance (Ω)	Distance(km)	Number of towers	Tower failure probability	Line Failure Probability
4-5	0.366	0.915	5	0.5296	0.7413
21-22	0.475	1.188	6	0.4686	0.7077
23-24	1.620	4.050	17	0.8332	0.9083
34-35	0.768	1.920	9	0.6126	0.7869

5.2.2 Integrated Response Results

The program goes through 5 iterations until convergence, when the optimized solution is obtained. The computation time is 894s, which is acceptable for a system operation problem. The illustration of preventive topology reconfiguration is shown in **Figure 5.7**. The system reconfiguration after preventive response is shown in **Figure 5.8**. To deal with the possible damage caused by windstorms, branch 23-24 and tie-branch 1 are open while tie-branch 2 and 3 are closed to guarantee the radial topology in preventive state.

To get better analysis of the system, it is reasonable to divide all the bus into four parts according to their location and the distribution of tie branches. Top left part has

bus 1~15, 68 and 69, while bus 16~29 is in top right part. The bottom left part consists of bus 30~50 and bottom right part has bus 51~67. The correspond total load of these four parts are 0.793MW, 0.790MW, 1.278MW and 1.178MW, respectively. Notice from **Table 5.6** that the maximum output of distributed generators which located in counterpart in the system is 2.2MW, 1.3MW, 1.3MW and 0.7MW. The right two parts can't provide enough power even when DG5 and DG6 are in fully output.

Branch 23-24 is considered as fragile lines with failure probability of 0.9083. Meanwhile, there is breakers in branch 23-24. It is logical to open it before event comes since it has such a great failure probability to cause damage after the event. Opening it in preventive state does no harm to the normal operation for the system since there are dispatchable resources such as generators and breakers. Branch 21-22 is also fragile lines with 0.7077 failure probability. Once the branch 21-22 is destroyed by windstorms, the top left part and top right part can no longer provide power to the bottom right part since the connectivity is damaged. However, the DGs in the bottom part cannot supply its own demand. Then it is reasonable and profitable to closed tie-branch 2 to reconstruct the connectivity of top left part and bottom right part. The existence of other two fragile lines doesn't influence the preventive reconfiguration since they are in the parts where power supply is sufficient. It is not economic to do other switching. In other words, the cost of doing other switching cannot is higher than the reduced cost in load shedding.
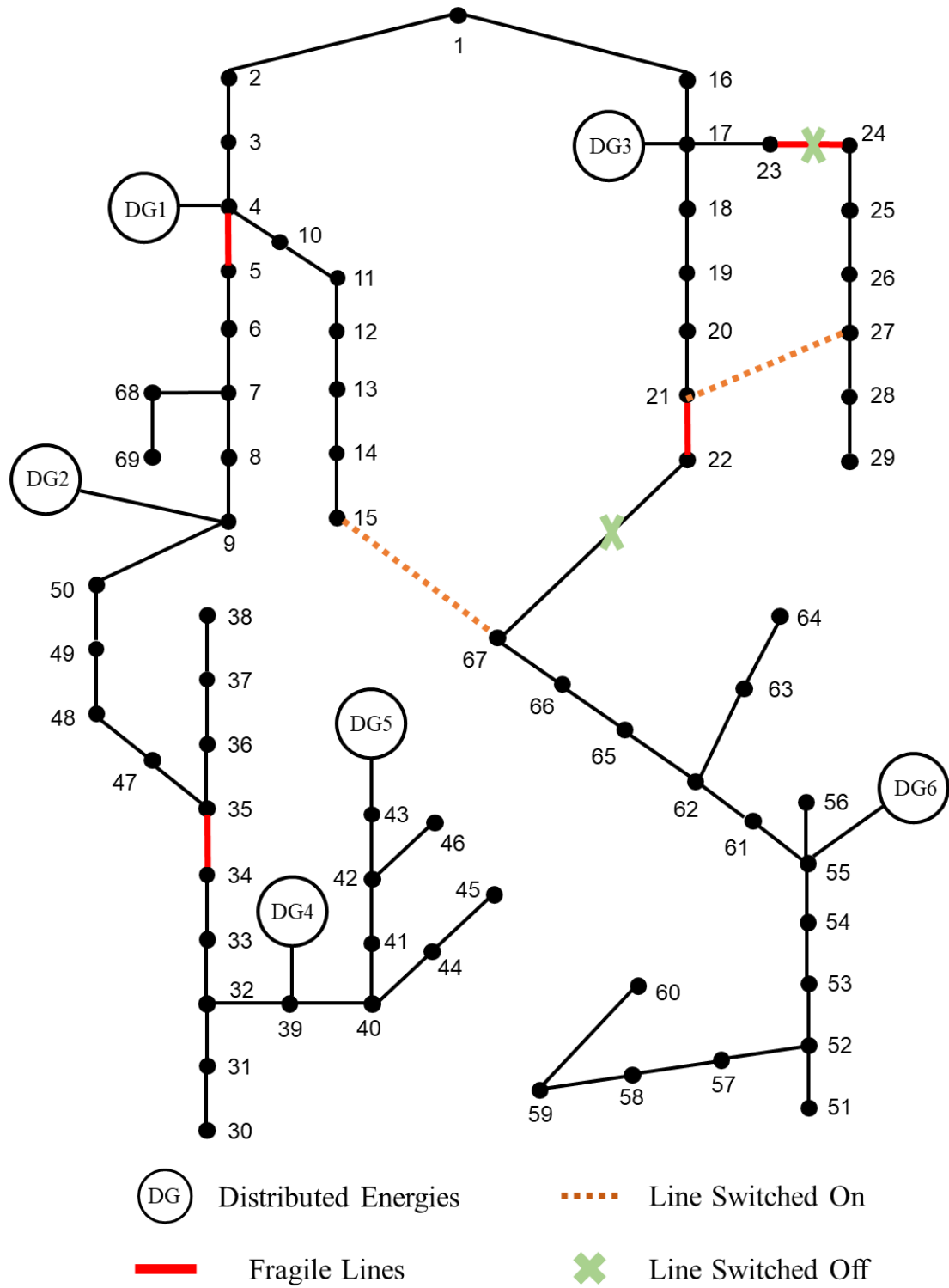
Figure 5.7 Illustration of topology reconfiguration in preventive response.
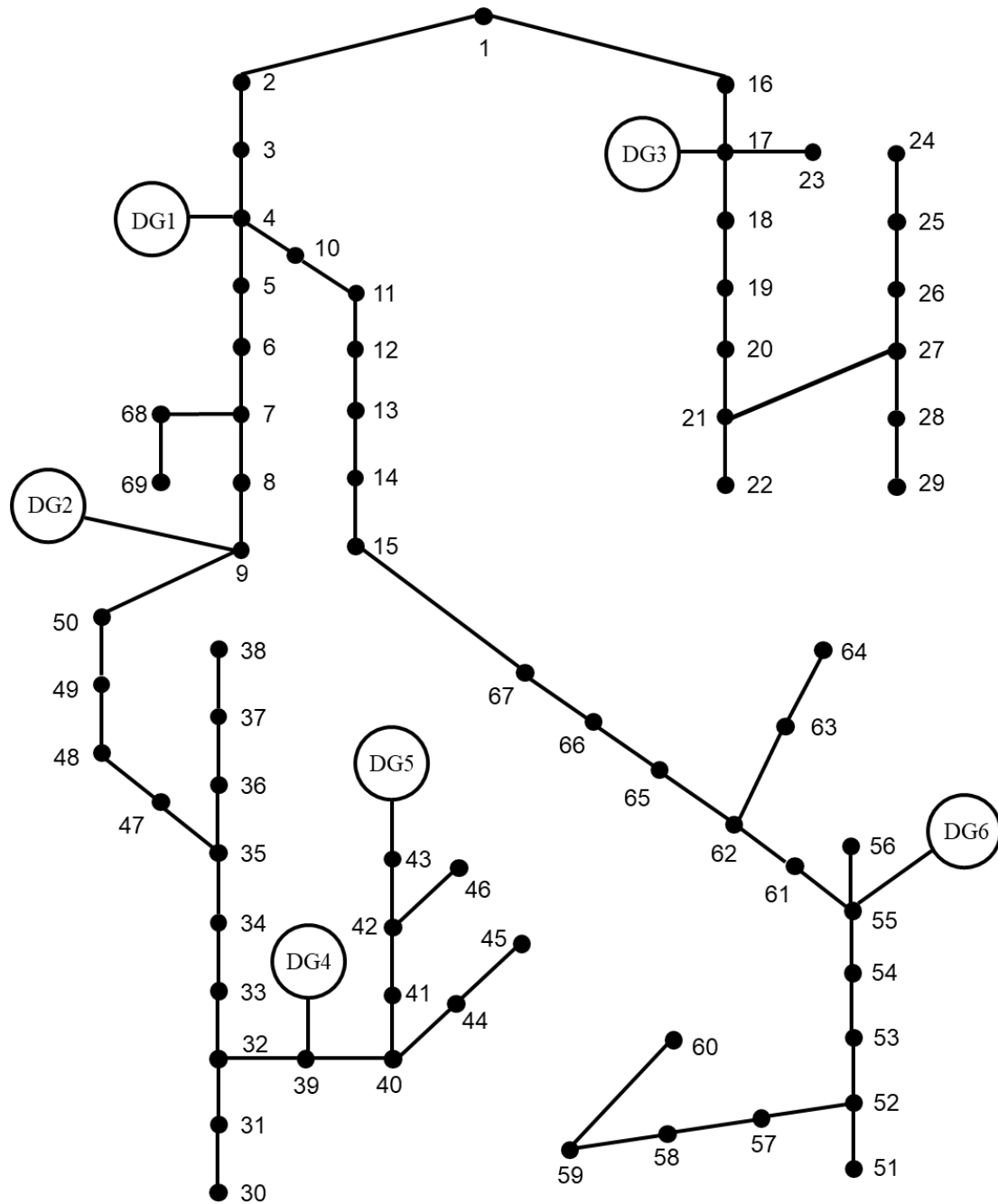
Figure 5.8 System topology after preventive response.

The expected total cost is $4,800, in which $1,110 is preventive reconfiguration cost and $3,659 refers to the expected load shedding cost considering all 16 possible scenarios for four fragile lines. The expected emergency switching cost is $41.

5.2.3 Scenario Comparison

According to the response that is deployed in the event, five scenarios are used to make comparison, same as previous study. The solution of five scenarios and the expected total cost is in **Table 5.8**.

<p align="center">**Table 5.8** Expected total cost and solution of five scenarios</p>

Scenario	*Pre-To*	*Em-Gr*	*Em-To*	Expected Total Cost ($)	Solution
1	✗	✗	✗	--	Only scenario 11, 12, 15 and 16 are feasible
2	✓	✗	✗	--	Only scenario 11, 12, 15 and 16 are feasible
3	✓	✓	✗	5,027	23-24 off, tie 1 off, tie 2 on, tie 3 on
4	✗	✓	✓	5,154	23-24 off, tie 1 off, tie 2 on, tie 3 on
5	✓	✓	✓	4,800	23-24 off, tie 1 off, tie 2 on, tie 3 on

The first two scenarios have no global solution in preventive response reconfiguration. Only several scenarios are feasible for scenario 1 and 2. It is because generator redispatch is not allowed in these two scenarios, which limit the ramping ability of distributed generators. When system operates in normal condition, the total load is supplied and the generator output is equal to or more than total load. However, the windstorms cause damage to system component. The only way to keep power balance is carrying out load shedding and the generator must be dispatched to be equivalent to reduced load. If no ramping is allowed, the power balance constraints and the ramping limit contradictory to each other, making the problem infeasible.

For scenario 3, 4 and 5, they are all feasible for all scenarios and have the same solution. Compare to scenario 3 and 4, scenario 5 has the least expected total cost

because preventive topology switching, emergency generator redispatch and emergency topology switching are all allowed in scenario 5, which is exactly integrated response in this thesis. The results show that the expected total cost can be minimized by utilizing all the responses, which reflects the correctness of the proposed optimization model. The expected total cost in scenario 3 is al little less than that in scenario 4. To explore the reason of that phenomenon, a detailed expected total cost analysis is shown in **Table 5.9**. Since the first two scenarios are not generally feasible, they are not included in the table.

Table 5.9 Detailed expected total cost analysis

Scenario	*Pre-To* Cost ($)	Expected Load shedding Cost ($)	Expected *Em-To* Cost ($)	Expected Total Cost ($)	Expected Load shedding (MW)
3	1,100	3,927	0	5,027	3.927
4	0	3,273	1,881	5,154	3.273
5	1,100	3,659	41	4,800	3.659

Notice that when it comes to expected load shedding cost, scenario 4 is the best. Load shedding cost is the product of amount of load curtailment and unit load shedding cost. It can represent distribution resilience level. Thus scenario 4 has the best resilience level. It shows the good performance of emergency topology switching in isolated distribution systems. And the comparison of scenario 3 and 5 also illustrate the importance of emergency topology switching. By deploying emergency switching, the expected load shedding cost reduced from $3,927 to %3,659 with the cost of only $41 expected emergency cost, which is absolutely cost-effective.

The comparison between scenario 1 and 5 shows that the proposed integrated response framework can effectively help to improve the system operation condition in

a minimum cost and the system resilience is also improved by reducing load shedding.
And the integrated response can improvement distribution system resilience while the
expected total cost is minimized.

5.2.4 Sensitivity Analysis

To further explore the performance of integrated response in variant operation
condition, parameter sensitivity analysis is done in this section. It should be mentioned
that the modified 69 bus system is isolated from the main grid and all the load is
supplied by DGs. In this circumstance, the availability and ramping ability of DGs is
essential to the distributed system resilience level.

The generator availability analysis is achieved by assuming that DG 1 is composed
of 12 identical fuel cells with maximum output of 0.1 MW each. **Figure 5.9** shows the
amount of load shedding when several fuel cells are unavailable.
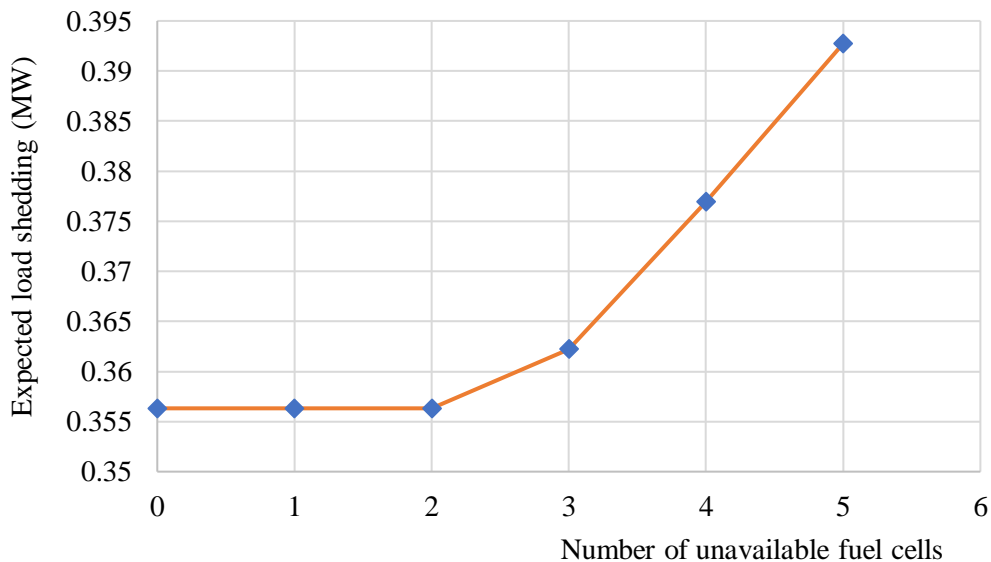
Figure 5.9 Expected load shedding under fuel cells unavailability.

It can be seen that the availability of distributed generators plays an importance role in isolated systems resilience. When the number of unavailable fuel cells are 0, 1 and 2, the expected load shedding doesn't change at all since the total amount of DGs output is far more than total load and other DGs can make up the lacking power. However, when the maximum DG1 output is less than 1.0MW, the expected load shedding increases dramatically and when there are more than 6 unavailable fuel cells, the problem has no solution. We mentioned that the amount of load curtailment represents the distribution system resilience level. Thus, the availability of DGs is essential to distributed system resilience.

Table 5.10 Emergency ramping limit sensitivity analysis.

Emergency Ramping Limit of DG 2 (MW/h)	Expected Total Cost ($)	Expected Load Shedding (MWh)
0.60	4,663	0.35632
0.59	4,663	0.35632
0.58	4,663	0.35632
0.57	4,667	0.35667
0.56	4,690	0.35675
0.55	4,706	0.36060
0.54	4,730	0.36294
0.53	4,800	0.36590
0.52	4,805	0.37050

Table 5.10 shows the expected total cost and expected load curtailment cost when DG 2 has different ramping limit. The duration of emergency response is set as 1 hour and since the distribution system is total supplied by distributed energies, the ramping ability influence the resilience of system. It is concluded that worse ramping ability not only increases the cost of integrated response but also make the system less resilient to windstorms.

5.3 Conclusion

The above two case studies on IEEE 33 bus system and modified 69 bus system illustrate the effectiveness and correctness of proposed integrated response framework and model. The two systems operate in connected mode and isolation mode, respectively. Distribution system operators can improve system resilience by employing the integrated response framework in a minimum cost in both modes. The main conclusions are listed as follows:

● Integrated response can improve distribution system resilience in a minimum cost in both connected system and isolated system.

● The effectiveness of integrated response is better than the individual preventive or emergency response.

● System parameters and abilities such as unit load shedding cost, ramping ability and generator availability influence the system resilience and expected total cost in different degree.

Chapter 6 Thesis conclusion and Future Work

This thesis focuses on using integrated response to boost distribution system resilience. The preventive response includes topology reconfiguration, generator redispatch, while emergency response consists of topology reconfiguration, generator redispatch and load shedding. Load shedding is not allowed in preventive state since the main function of distribution system is to supply the load when it is in normal condition.

The thesis first proposes a two-stage integrated response framework to mitigate the impact of extreme weathers especially windstorms. Then a two-stage mix-integer linear programming is formulated as the core of the framework since topology reconfiguration is involved in both preventive and emergency state. Progressive hedging algorithm is utilized to solve the two-stage stochastic model due to its good performance in integer-involved two-stage problem. Two case studies are carried out to verify the proposed method.

IEEE 33 bus system is set to connect to the main grid with seven controllable distributed generators. The solution of integrated response is first presented by comparing the initial system reconfiguration and preventive state topology. Line7-8 is open and tie-branch 21-8 is closed in preventive response to cope with the up-coming windstorms, which provides a possible solution for distribution system operators to deal with the extreme weather events. The expected total cost is $10,070. Five scenarios are designed to make the problem clear and scenario comparison shows that integration of preventive response and emergency response can improve distribution resilience by

reducing the amount of load curtailment in a minimum cost, and the effect of integrated response is better than either single one. To further explore the impact of parameter changing to the problem solution, sensitivity analysis is carried out under different unit load shedding cost, ramping limit and forecast wind speed. The conclusion is that the expected total cost increases when unit load shedding cost increases and they are in linear relationship. Either the relax in preventive ramping limit or emergency ramping limit reduces the total but to a certain extent.

The modified 69 bus system operates in an islanded mode, in which all the load is satisfied by distributed energies. Line 23-24 and tie-branch 1 are open while tie-branch 2 and 3 are closed in preventive response when integrated response is allowed. The system resilience is improved compared to the system without response, when the system may break in several scenarios. The sensitivity analysis is done to emphasize the importance of availability and ramping ability of DGs in distribution systems. It is concluded that either the decrease in ramping ability or unavailable generators increases the risk of load shedding and expected total cost, then the system resilience is decreased.

The case study shows that integrated response can improve distribution system resilience in a minimum cost in both connected system and isolation system. The integrated response has the least expected total cost compared to individual preventive or emergency response. System parameters and abilities such as unit load shedding cost, ramping ability and generator availability influence the system resilience and expected total cost in different degree.

As is mention before, this thesis doesn't consider the uncertainty of distributed

energies and weather event such as wind speed, which could be carried out in the future work about stochastic problems. The output of renewable energies and actual weather condition may differ from estimation. Besides, the computation burden increases with the increase of fragile lines. Some heuristic algorithm such as genetic algorithm could be used in solving such problems.

Furthermore, the proposed work could also be extended to address the emerging cyber-physical resiliency when the power grid is under the potential cyber-physical attacks.

Appendices

Appendix A: The 33-bus distribution test system
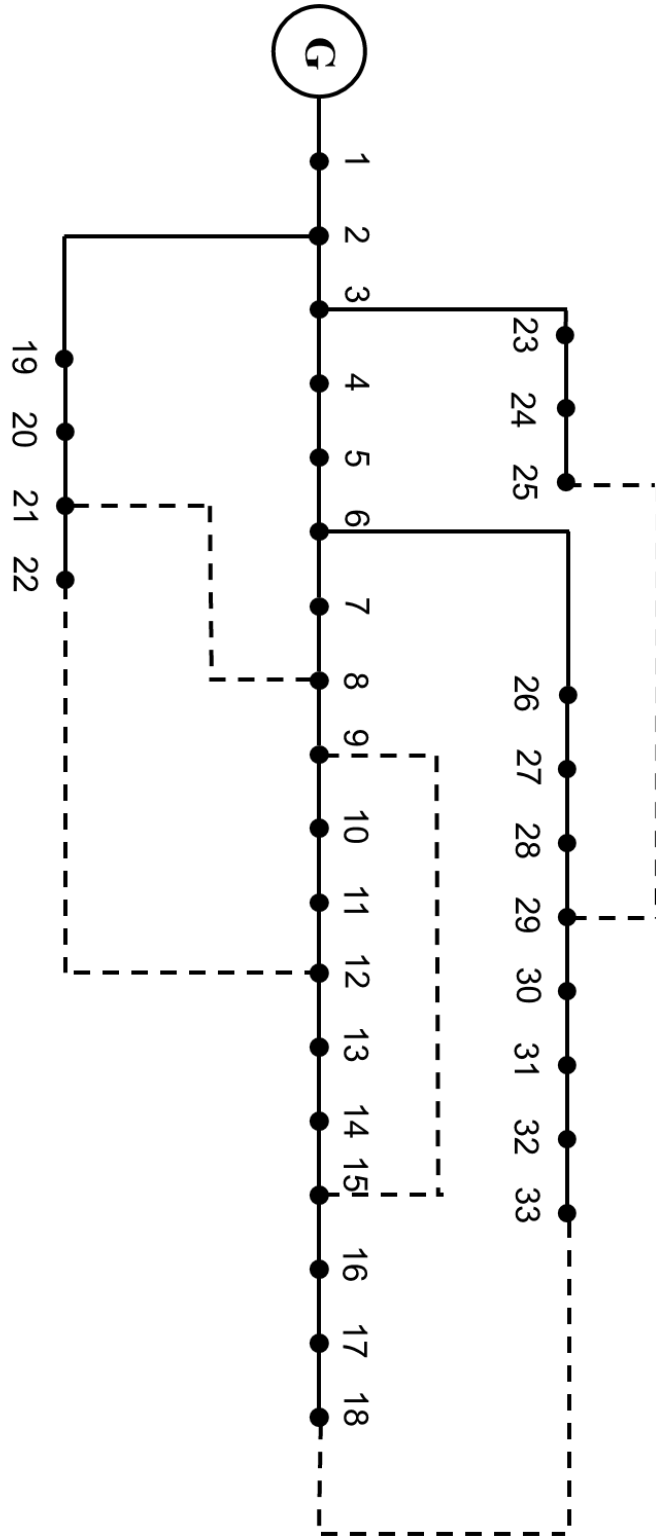
Appendix B: System data for 33 bus radial distribution system ('*' denotes a tie-bracnch)

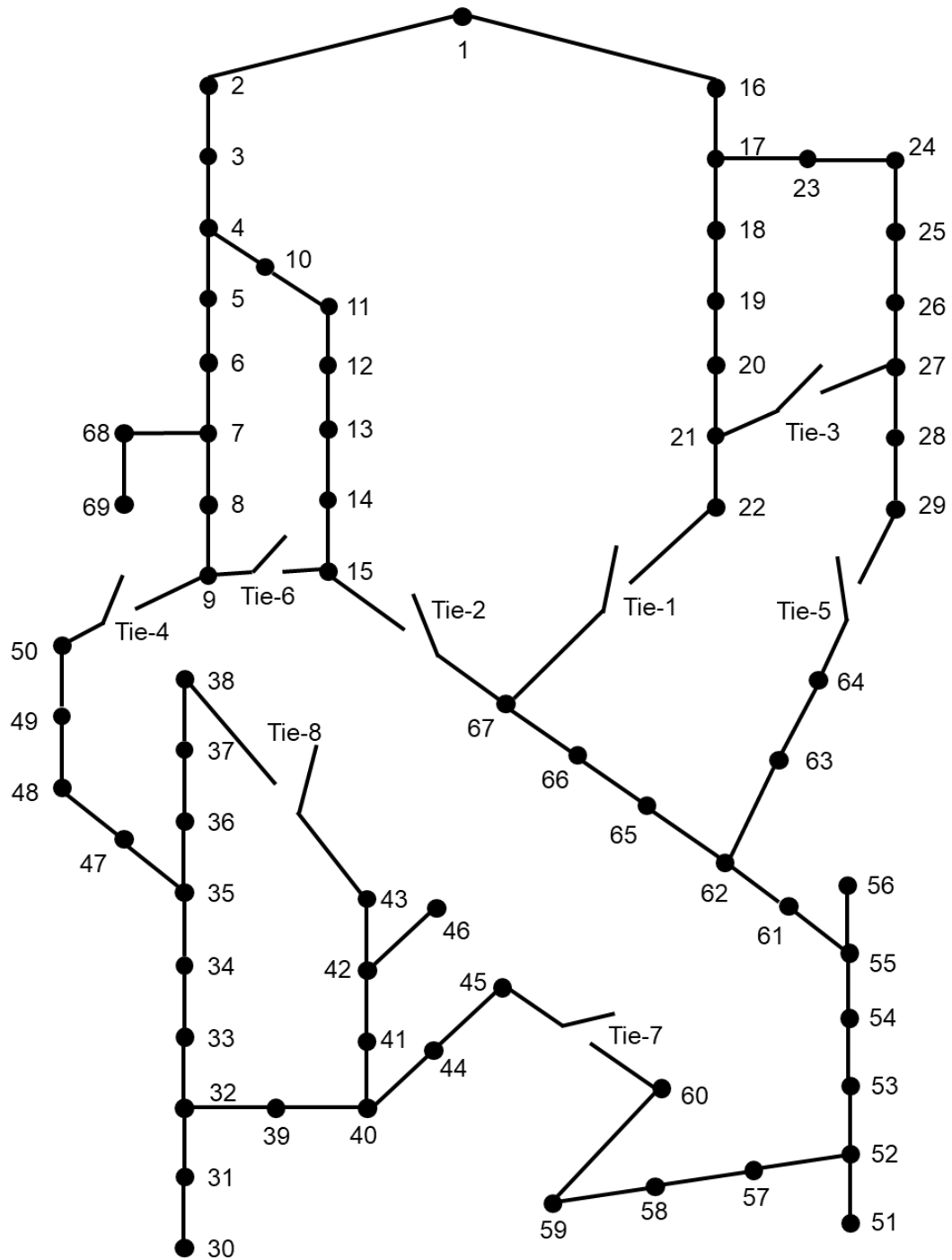| Number	Sending Bus	Receiving Bus	Resistance (Ω)	Reactance (Ω)	Nominal Load at Receiving Bus	
					P (kW)	Q (kVAr)
1	1	2	0.0922	0.047	100	60
2	2	3	0.493	0.2511	90	40
3	3	4	0.366	0.1864	120	80
4	4	5	0.3811	0.1941	60	30
5	5	6	0.819	0.707	60	20
6	6	7	0.1872	0.6188	200	100
7	7	8	0.7114	0.2351	200	100
8	8	9	1.03	0.74	60	20
9	9	10	1.044	0.74	60	20
10	10	11	0.1966	0.065	45	30
11	11	12	0.3744	0.1298	60	35
12	12	13	1.468	1.155	60	35
13	13	14	0.5416	0.7129	120	80
14	14	15	0.591	0.526	60	10
15	15	16	0.7463	0.545	60	20
16	16	17	1.289	1.721	60	20
17	17	18	0.732	0.574	90	40
18	2	19	0.164	0.1565	90	40
19	19	20	1.5042	1.3554	90	40
20	20	21	0.4095	0.4784	90	40
21	21	22	0.7089	0.9373	90	40
22	3	23	0.4512	0.3083	90	50
23	23	24	0.898	0.7091	420	200
24	24	25	0.896	0.7011	420	200
25	6	26	0.203	0.1034	60	25
26	26	27	0.2842	0.1447	60	25
27	27	28	1.059	0.9337	60	20
28	28	29	0.8042	0.7006	120	70
29	29	30	0.5075	0.2585	200	600
30	30	31	0.9744	0.963	150	70
31	31	32	0.3105	0.3619	210	100
32	32	33	0.341	0.5302	60	40
33*	21	8	2	2		
34*	9	15	2	2		
35*	12	22	2	2		
36*	18	33	0.5	0.5		
37*	25	29	0.5	0.5		

Appendix C: Modified 69-bus distribution test system

Appendix D: System data for 69 bus radial distribution system ('*' denotes a tie-bracnch)

Number i	Sending Bus	Receiving Bus	Resistance (Ω)	Reactance (Ω)	Nominal Load at Bus i	
					P (kW)	Q (kVAr)
1	1	2	1.097	1.074	0	0
2	2	3	1.463	1.432	120.0	108.0
3	3	4	0.731	0.716	72.0	48.0
4	4	5	0.366	0.358	180.0	156.0
5	5	6	1.828	1.79	90.0	60.0
6	6	7	1.097	1.074	21.6	13.0
7	7	8	0.731	0.716	21.6	17.0
8	8	9	0.731	0.716	15.6	12.0
9	4	10	1.08	0.734	19.0	13.0
10	10	11	1.62	1.101	24.0	12.0
11	11	12	1.08	0.734	19.2	11.0
12	12	13	1.35	0.917	60.0	48.0
13	13	14	0.81	0.55	126.0	108.0
14	14	15	1.944	1.321	30.0	18.0
15	7	68	1.08	0.734	48.0	30.0
16	68	69	1.62	1.101	120.0	72.0
17	1	16	1.097	1.074	48.0	36.0
18	16	17	0.366	0.358	72.0	36.0
19	17	18	1.463	1.432	48.0	30.0
20	18	19	0.914	0.895	18.0	11.0
21	19	20	0.804	0.787	15.6	8.4
22	20	21	1.133	1.11	36.0	24.0
23	21	22	0.475	0.465	108.0	60.0
24	17	23	2.214	1.505	60.0	36.0
25	23	24	1.62	1.11	72.0	48.0
26	24	25	1.08	0.734	120.0	96.0
27	25	26	0.54	0.367	96.0	78.0
28	26	27	0.54	0.367	120.0	72.0
29	27	28	1.08	0.734	120.0	66.0
30	28	29	1.08	0.734	144.0	84.0
31	30	31	0.731	0.716	126.0	84.0
32	31	32	0.731	0.716	96.0	60.0
33	32	33	0.804	0.787	72.0	48.0
34	33	34	1.17	1.145	15.6	9.6
35	34	35	0.768	0.752	19.2	11.8
36	35	36	0.731	0.716	60.0	36.0
37	36	37	1.097	1.074	48.0	33.6

38	37	38	1.463	1.432	72.0	48.0
39	32	39	1.08	0.734	48.0	36.0
40	39	40	0.54	0.367	36.0	30.0
41	40	41	1.08	0.734	180.0	120.0
42	41	42	1.836	1.248	72.0	42.0
43	42	43	1.296	0.881	144.0	84.0
44	40	44	1.188	0.807	108.0	72.0
45	44	45	0.54	0.367	21.6	12.0
46	42	46	1.08	0.734	19.2	12.0
47	35	47	0.54	0.367	120.0	60.0
48	47	48	1.08	0.734	72.0	48.0
49	48	49	1.08	0.734	108.0	84.0
50	49	50	1.08	0.734	122.4	79.2
51	51	52	1.463	1.432	120.0	84.0
52	52	53	1.463	1.432	168.0	108.0
53	53	54	0.914	0.895	72.0	48.0
54	54	55	1.097	1.074	24.0	13.2
55	55	56	1.097	1.074	48.0	36.0
56	52	57	0.27	0.183	43.2	28.8
57	57	58	0.27	0.183	36.0	24.0
58	58	59	0.81	0.55	51.6	36.0
59	59	60	1.296	0.881	96.0	60.0
60	55	61	1.188	0.807	288.0	144.0
61	61	62	1.188	0.807	150.0	132.0
62	62	63	0.81	0.55	30.0	12.0
63	63	64	1.62	1.101	12.0	6.0
64	62	65	1.08	0.734	180.0	156.0
65	65	66	0.54	0.367	60.0	36.0
66	66	67	1.08	0.734	36.0	24.0
67*	22	67	0.381	0.2445	156.0	144.0
68*	67	15	0.454	0.363	180.0	156.0
69*	21	27	0.254	0.203	30.0	18.0
70*	9	50	0.681	0.5445		
71*	29	64	0.681	0.5445		
72*	9	15	0.454	0.3630		
73*	45	60	0.254	0.203		
74*	43	38	0.254	0.2030		

References

[1] F. Estrada, W. Botzen, and R. Tol, "Economic losses from US hurricanes consistent with an influence from climate change," *Nature Geosci.*, vol. 8, pp. 880–884, Nov. 2015.

[2] R. E. Brown, "Hurricane hardening efforts in Florida," *Proc. IEEE Power Energy Soc. Gen. Meeting — Conversion Del. Elect. Energy 21st Century*, Jul. 2008, pp. 1–7.

[3] "Hurricane sandy event analysis report," *North Amer. Electr. Rel. Corp.*, Atlanta, GA, USA, Jan. 2014.

[4] "Economic benefits of increasing electric grid resilience to weather outages," White House, *Tech. Rep.*, Jul. 2013.

[5] A. Gholami, F. Aminifar, and M. Shahidehpour, "Front lines against the darkness: Enhancing the resilience of the electricity grid through microgrid facilities," *IEEE Electrific. Mag.*, vol. 4, no. 1, pp. 18–24, Mar. 2016.

[6] M. Panteli, D. N. Trakas, P. Mancarella and N. D. Hatziargyriou, "Power Systems Resilience Assessment: Hardening and Smart Operational Enhancement Strategies," *Procs. IEEE*, vol. 105, no. 7, pp. 1202-1213, Jul. 2017.

[7] T. Liacco, "The adaptive reliability control system," *IEEE Trans. Power App. Syst.*, vol. 5, no. PAS-86, pp. 517–531, May 1967.

[8] G. Huang, J. Wang, C. Chen, J. Qi and C. Guo, "Integration of Preventive and Emergency Responses for Power Grid Resilience Enhancement," *IEEE Trans. Power Syst.*, vol. 32, no. 6, pp. 4451-4463, Nov. 2017.

[9] A.Kenward and U. Raja, "Blackout: Extreme weather, climate change and power outages," *Tech. Rep.*, Apr. 2014. [Online]. Available: https://www.ourenergypolicy.org/wp-content/uploads/2014/04/climate-central.pdf

[10] C. S. Holling, "Resilience and stability of ecological systems," Ecology, vol. 4, no. 1, pp. 1–23, 1973.

[11] U.S. Department of Energy. 2009 smart grid system report [R]. Washington, D.C.: U.S. Department of Energy, 2009

[12] Presidential Policy Directive (PPD) 21, The White House, Washington, DC, USA, 2013.

[13] M. Chaudry et al., Building a Resilient UK Energy System. London,U.K.: UK Energy Research Center (UKERC), Apr. 14, 2011.

[14] Third UN World Conference on Disaster Risk Reduction, United Nations Office for Disaster Risk Reduction (UNISDR), Sendai, Japan, 2015

[15] M. Panteli and P. Mancarella, "The Grid: Stronger, Bigger, Smarter? Presenting a Conceptual Framework of Power System Resilience," *IEEE Power Energy Mag.*, vol. 13, no. 3, pp. 58-66, May-Jun. 2015.

[16] Z. Bie, Y. Lin, G. Li and F. Li, "Battling the Extreme: A Study on the Power System Resilience," *Procs. IEEE*, vol. 105, no. 7, pp. 1253-1266, Jul. 2017.

[17] S. McManus, E. Seville, D. Brunsdon, and J. Vargo, "Resilience management: A framework for assessing and improving the resilience of organisations," *Resilient Organ. Res. Rep.*, vol. 1, pp. 1–79, 2007.

[18] P. E. Roege, Z. A. Collier, J. Mancillas, J. A. McDonagh, and I. Linkov, "Metrics for energy resilience," *Energy*

Policy, vol. 72, pp. 249–256, Sep. 2014.

[19] P. M. Orencio and M. Fujii, "A localize disaster-resilience index to assess coastal communities based on an analytic hierarchy process (AHP)," *Int. J. Disaster Risk Reduct.*, vol. 3, pp. 62–75, Mar. 2013.

[20] K. Alvehag and L. Soder, "A Reliability Model for Distribution Systems Incorporating Seasonal Variations in Severe Weather," *IEEE Trans. Power Del.*, vol. 26, no. 2, pp. 910-919, Apr. 2011.

[21] M. Schlapfer and P. Mancarella, "Probabilistic Modeling and Simulation of Transmission Line Temperatures Under Fluctuating Power Flows," *IEEE Trans. Power Del.*, vol. 26, no. 4, pp. 2235-2243, Oct. 2011.

[22] M. Panteli and P. Mancarella, "Modeling and Evaluating the Resilience of Critical Electrical Power Infrastructure to Extreme Weather Events," *IEEE Systems Journ.*, vol. 11, no. 3, pp. 1733-1742, Sept. 2017.

[23] R. Rocchetta, E. Zio and E. Patelli, E. A Power-Flow Emulator Approach for Resilience Assessment of Repairable Power Grids subject to Weather-Induced Failures and Data Deficiency *Appl. Energy*, vo. 210, pp. 339-35, 2018.

[24] M. Ouyang and L. Duenas-Osorio, "Time-dependent resilience assessment and improvement of urban infrastructure systems," *Chaos*, vol. 22, Sep. 2012, Art. no. 033122.

[25] D. A. Reed, K. C. Kapur, and R. D. Christie, "Methodology for assessing the resilience of networked infrastructure," *IEEE Systems Journ.*, vol. 3, no. 2, pp. 174–180, May 2009.

[26] R. K. Mathew, S. Ashok, and S. Kumaravel, "Resilience assessment of Electric Power Systems: A scoping study," *2016 IEEE Students' Conf. Electr. Electron. Comput. Sci. SCEECS 2016*, pp. 1–4, 2016

[27] Z. Li, M. Shahidehpour, F. Aminifar, A. Alabdulwahab and Y. Al-Turki, "Networked Microgrids for Enhancing the Power System Resilience," *Procs. IEEE*, vol. 105, no. 7, pp. 1289-1310, Jul. 2017.

[28] M. H. Amirioun, F. Aminifar and H. Lesani, "Towards Proactive Scheduling of Microgrids Against Extreme Floods," *IEEE Trans. Smart Grid*, vol. 9, no. 4, pp. 3900-3902, Jul. 2018.

[29] M. Panteli, P. Mancarella, D. N. Trakas, E. Kyriakides and N. D. Hatziargyriou, "Metrics and Quantification of Operational and Infrastructure Resilience in Power Systems," *IEEE Trans. Power Syst.*, vol. 32, no. 6, pp. 4732-4742, Nov. 2017.

[30] P. J. Maliszewski and C. Perrings, "Factors in the resilience of electrical power distribution infrastructures," *Appl. Geogr.*, vol. 32, no. 2, pp. 668–679, 2012.

[31] U.S. Department of Energy, Hardening and Resiliency: U.S. Energy Industry Response to Recent Hurricane Seasons, *Tech. Rep.*, Aug. 2010 [Online]. Available: http://www.oe.netl.doe.gov/docs/HR-Report-final-081710.pdf

[32] W. Yuan, J. Wang, F. Qiu, C. Chen, C. Kang and B. Zeng, "Robust Optimization-Based Resilient Distribution Network Planning Against Natural Disasters," *IEEE Trans. Smart Grid*, vol. 7, no. 6, pp. 2817-2826, Nov. 2016.

[33] C. Shao, M. Shahidehpour, X. Wang, X. Wang and B. Wang, "Integrated Planning of Electricity and Natural Gas Transportation Systems for Enhancing the Power Grid Resilience," *IEEE Trans. Power Syst.*, vol. 32, no. 6, pp. 4418-4429, Nov. 2017.

[34] S. Ma, L. Su, Z. Wang, F. Qiu and G. Guo, "Resilience Enhancement of Distribution Grids Against Extreme Weather Events," *IEEE Trans. Power Syst.*, vol. 33, no. 5, pp. 4842-4853, Sept. 2018.

[35] X. Wang, Z. Li, M. Shahidehpour and C. Jiang, "Robust Line Hardening Strategies for Improving the Resilience of Distribution Systems With Variable Renewable Resources," *IEEE Trans. Sust. Energy*, vol. 10, no. 1, pp. 386-395, Jan. 2019.

[36] C. He, C. Dai, L. Wu and T. Liu, "Robust Network Hardening Strategy for Enhancing Resilience of Integrated Electricity and Natural Gas Distribution Systems Against Natural Disasters," *IEEE Trans. Power Syst.*, vol. 33, no. 5, pp. 5787-5798, Sept. 2018.

[37] S. Ma, B. Chen and Z. Wang, "Resilience Enhancement Strategy for Distribution Systems Under Extreme Weather Events," *IEEE Trans. Smart Grid*, vol. 9, no. 2, pp. 1442-1451, Mar. 2018.

[38] M. Zare, A. Abbaspour, M. Fotuhi-Firuzabad and M. Moeini-Aghtaie, "Increasing the resilience of distribution systems against hurricane by optimal switch placement," *2017 Conference on Electrical Power Distribution Networks Conference (EPDC)*, Semnan, 2017, pp. 7-11.

[39] M. Zare-Bahramabadi, A. Abbaspour, M. Fotuhi-Firuzabad and M. Moeini-Aghtaie, "Resilience-based framework for switch placement problem in power distribution systems," *IET Gener. Transm. Distrib.*, vol. 12, no. 5, pp. 1223-1230, 13 3 2018.

[40] M. Panteli, D. N. Trakas, P. Mancarella and N. D. Hatziargyriou, "Boosting the Power Grid Resilience to Extreme Weather Events Using Defensive Islanding," *IEEE Trans. Smart Grid*, vol. 7, no. 6, pp. 2913-2922, Nov. 2016.

[41] M. Al Owaifeer and M. Al-Muhaini, "MILP-based technique for smart self-healing grids," *IET Gener. Transm. Distrib.*, vol. 12, no. 10, pp. 2307-2316, 29 5 2018.

[42] M. H. Amirioun, F. Aminifar and H. Lesani, "Resilience-Oriented Proactive Management of Microgrids Against Windstorms," *IEEE Trans. Power Syst.*, vol. 33, no. 4, pp. 4275-4284, Jul. 2018.

[43] C. Chen, J. Wang, F. Qiu and D. Zhao, "Resilient Distribution System by microgrids Formation After Natural Disasters," *IEEE Trans. Smart Grid*, vol. 7, no. 2, pp. 958-966, Mar. 2016.

[44] X. Liu, M. Shahidehpour, Z. Li, X. Liu, Y. Cao and Z. Bie, "Microgrids for Enhancing the Power Grid Resilience in Extreme Conditions," *IEEE Trans. Smart Grid*, vol. 8, no. 2, pp. 589-597, Mar. 2017.

[45] Multi-Resolution Land Characteristics Consortium, National Land Cover Database (NLCD) [Online]. Available: http://www.mrlc.gov/

[46] M. Panteli, "Impact of ICT reliability and situation awareness on power system blackouts," Ph.D. dissertation, Univ. Manchester, Manchester, U.K., 2013.

[47] National Weather Service: National Hurrican Center, National Oceanic and Atmospheric Administration (NOAA) Hurricane Database [Online]. Available: http://www.nhc.noaa.gov/

[48] National Weather Service: Advanced Hydrologic Prediction Service, National Oceanic and Atmospheric Administration (NOAA) Precipitation Database [Online]. Available: http://water.weather.gov/precip/

[49] L. Che and M. Shahidehpour, "Adaptive Formation of Microgrids With Mobile Emergency Resources for Critical Service Restoration in Extreme Conditions," *IEEE Trans. Power Syst.*, vol. 34, no. 1, pp. 742-753,

Jan. 2019.

[50] S. Lei, J. Wang, C. Chen and Y. Hou, "Mobile Emergency Generator Pre-Positioning and Real-Time Allocation for Resilient Response to Natural Disasters," *IEEE Trans. Smart Grid*, vol. 9, no. 3, pp. 2030-2041, May 2018.

[51] J. Kim and Y. Dvorkin, "Enhancing Distribution System Resilience with Mobile Energy Storage and Microgrids," *IEEE Trans. Smart Grid*.

[52] J. Kim and Y. Dvorkin, "Enhancing Distribution Resilience with Mobile Energy Storage: A Progressive Hedging Approach," *2018 IEEE Power & Energy Society General Meeting (PESGM)*, Portland, OR, 2018, pp. 1-5.

[53] B. Zhang, P. Dehghanian and M. Kezunovic, "Optimal Allocation of PV Generation and Battery Storage for Enhanced Resilience," *IEEE Trans. Smart Grid*, vol. 10, no. 1, pp. 535-545, Jan. 2019.

[54] Y. Xu *et al*., "DGs for Service Restoration to Critical Loads in a Secondary Network," *IEEE Trans. Smart Grid*, vol. 10, no. 1, pp. 435-447, Jan. 2019.

[55] S. Poudel and A. Dubey, "Critical Load Restoration Using Distributed Energy Resources for Resilient Power Distribution System," *IEEE Trans. Power Systs.*, vol. 34, no. 1, pp. 52-63, Jan. 2019.

[56] J.-P. Watson and D. L. Woodruff, "Progressive hedging innovations for a class of stochastic mixed-integer resource allocation problems," *Comp. Manag. Sci.*, vol. 8, no. 4, pp. 355–370, 2011.

[57] P. A. Trodden, W. A. Bukhsh, A. Grothey, and K. I. M. McKinnon, "Optimization-based islanding of power networks using piecewise linear AC power flow," *IEEE Trans. Power Syst.*, vol. 29, no. 3, pp. 1212–1220, May 2014.

[58] M. E. Baran and F. F.Wu, "Network reconfiguration in distribution systems for loss reduction and load balancing," *IEEE Trans. Power Del.*, vol.4, no. 2, pp. 1401–1407, Apr. 1989.

[59] A. Shafieezadeh, U. P. Onyewuchi, M. M. Begovic, and R. DesRoches, "Age-dependent fragility models of utility wood poles in power distribution networks against extreme wind hazards," *IEEE Trans. Power Del.*, vol. 29, no. 1, pp. 131–139, Feb. 2014.

[60] D. Das, "Reconfiguration of distribution system using fuzzy multi-objective approach," *Int. J. Elect. Power Energy Syst.*, vol. 28, no. 5, pp. 331–338, Jun. 2006.